Preprints (www.preprints.org) | NOT PEER-REVIEWED | Posted: 4 May 2018 doi:10.20944/preprints201805.0085.v1

Peer-reviewed version available at Pharmaceuticals 2018, 11, 59; doi:10.3390/ph11020059

Article

Synthesis, Biological Evaluation and Molecular Docking Studies of the 7-Acetamido Substituted 2-Aryl-5-bromo-3-trifluoroacetylindoles as Potential Inhibitors of Tubulin Polymerization

Malose J. Mphahlele [1]* and Nishal Parbhoo [2]

[1] Department of Chemistry, College of Science, Engineering and Technology, University of South Africa, Private Bag X06, Florida 1710, South Africa

[2] Department of Life & Consumer Sciences, College of Agriculture and Environmental Sciences, University of South Africa, Private Bag X06, Florida 1710, South Africa. E-mail: parbhn1@unisa.ac.za

* Correspondence: mphahmj@unisa.ac.za; Tel.: +27-11-670-301

Abstract: Structurally related 7-acetyl-2-aryl-5-bromoindoles **2a–d** and the 7-acetamido-2-aryl-5-bromoindoles **4a–d** as well as their corresponding 3-trifluoroacetyl–substituted derivatives **5a–d** and **5e–h** were evaluated for potential antigrowth effect *in vitro* against the human lung cancer (A549) and cervical cancer (HeLa) cells. All of the 3-trifluoroacetyl–substituted 7-acetamido-2-aryl-5-bromoindoles **5e–h** were found to be more active against both cell lines when compared to the chemotherapeutic drug, Melphalan. The most active compound **5g** induced apoptosis in a caspase dependent manner for both cell lines. Compounds **5e–h** were found to significantly inhibit tubulin polymerization. Molecular docking of **5g** into the colchicine-binding site suggests that the compounds bind to tubulin by different type of interactions including pi-alkyl, amide-pi stacked and alkyl interactions as well as hydrogen bonding with the protein residues to elicit anticancer activity.

Keywords: 7-acetamido-2-aryl-5-bromoindoles, trifluoroacetylation; cytotoxicity; apoptosis; tubulin polymerization; molecular docking

1. Introduction

Microtubule targeting agents have an established history of utility in the treatment of cancer and have been instrumental as biological probes to identify the nature of tubulin and the role of tubulin dynamics in mitosis [1]. Colchicine is known to bind tubulin and block the formation of microtubules while other anticancer agents stabilize the tubulin structure and therefore prevent microtubule disassembly [2]. Nitrogen-containing heterocycles such as indoles with anticancer properties have potential to inhibit tubulin polymerization by binding to colchicine-binding site [3-5]. The methoxy-substituted 2-aryl-3-

© 2018 by the author(s). Distributed under a Creative Commons CC BY license.

Preprints (www.preprints.org) | NOT PEER-REVIEWED | Posted: 4 May 2018 doi:10.20944/preprints201805.0085.v1

Peer-reviewed version available at Pharmaceuticals 2018, 11, 59; doi:10.3390/ph11020059

formylindoles (**a**) shown in Figure 1, for example, have been found to completely block the microtubule assembly at micromolar concentrations, which suggests a correlation between cytotoxicity and the microtubule system [3]. Structure–activity relationship (SAR) studies of indole derivatives revealed that a hydrogen bond donor NH at position 1 is essential for their antiproliferative activity [3]. A nitrogen-containing group on the fused benzo ring of the indole derivatives, on the other hand, was found to lead to increased cytotoxicity against the HeLa and A549 cell lines as well as HIV-1 inhibition activity [6]. Likewise, the presence of a lipophilic bromine atom on the fused benzo ring of an indole framework was found to impart significant anti-tumour activity in both the synthetic [7] and the naturally [8] occurring indole derivatives. Aplicyanin A (**b**) shown in Figure 1, for example, is a 5-bromoindole–based compound isolated from ascidian *Aplidium cyaneum* and this compound has been found to exhibit increased antiproliferative activity against MDA-MB-231, A549 and HT-29 cancer cell lines [8]. A hydrogen bond acceptor such as a formyl group at position 3 of the indole framework of compound (**a**), for example, facilitates interaction with biological receptors and therefore enhance anticancer activity [9]. Although substitution of a trifluoroacetyl group is not a common practice in medicinal chemistry, Thomas *et al.* have previously observed that *N*-[(5-{[(4-methylphenyl)sulfonyl]amino}-3-(trifluoroacetyl)-1*H*-indol-1-yl)acetyl]-*L*-leucine (NTRC-824) shown in Figure 1, which was isolated as an impurity was 90-fold more active (IC_{50} = 38 nM) and selective for the neurotesin receptor type 2 (NTS2 *versus* NTS1) than the expected C-3 unsubstituted analogue (IC_{50} = 3322 nM) [10]. The enhanced activity of NTRC-824 is presumably due to the increased electron withdrawing effect of the trifluoromethyl group, which has been found to generally increase the lipophilicity, metabolic stability and activity profile compared to that of the 3-unsubstituted or 3-acetyl analogues [2,11-13].

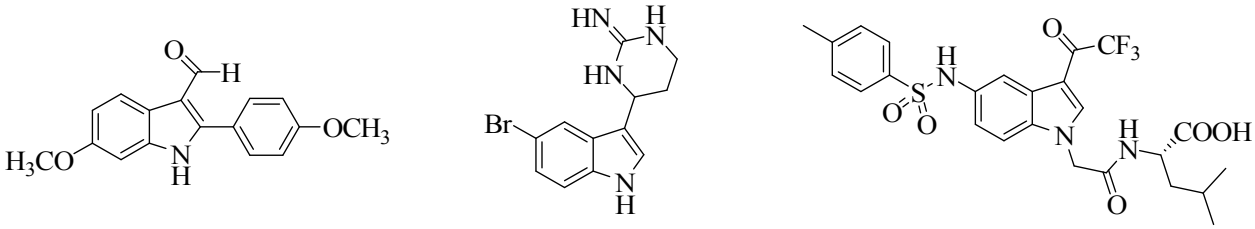

2-Aryl-3-formylindole (**a**) Aplicyanin A (**b**) NTRC-824 (**c**)

Figure 1: Structures of 3-formyl substituted 2-arylindole (**a**), aplicyanin A (**b**) and NTRC-824 (**c**)

We considered the antiproliferative properties of the 2-arylindoles [14] in combination with the above literature SAR analysis and decided to introduce a trifluoroacetyl group at the C-3 position of the 7-acetyl-2-aryl-5-bromoindoles and the 7-acetamido-2-aryl-5-bromoindoles. The main aim was to evaluate these polysubstituted indoles and their corresponding 3-trifluoroacetyl–substituted derivatives for anti-growth properties against the human lung cancer (A549) and cervical cancer (HeLa) cell lines. The pro-apoptotic properties of the analogous indole-3-carbinol [15] encouraged us to elucidate their mechanism of cancer cell death and for their ability to inhibit tubulin polymerization. The structure activity relationship (SAR) of the prepared compounds against these cell lines was studied with respect to the nature of substituent at the 2-, 3- and 7-position of the 5-bromoindole framework to correlate between both structural variations and cytotoxicity.

Preprints (www.preprints.org) | NOT PEER-REVIEWED | Posted: 4 May 2018 doi:10.20944/preprints201805.0085.v1

Peer-reviewed version available at Pharmaceuticals 2018, 11, 59; doi:10.3390/ph11020059

2. Results and Discussion

2.1 Chemistry

The 3-arylalkynylated 2-amino-5-bromoacetophenone derivatives **1a–d** were subjected to palladium chloride-mediated *endo-dig* cyclization to afford the 7-acetyl-2-aryl-5-bromoindoles **2a–d** in high yields (Table 1, Scheme 1). Oximation of indoles **2a–d** with hydroxylamine hydrochloride in the presence of pyridine in ethanol under reflux afforded the corresponding oxime derivatives **3a–d**. The ^{1}H-NMR spectra of the indole derivatives **2a–d** revealed the presence of two singlets around δ 6.90 and 11.10 ppm, which correspond to H-3 and NH, respectively. The oxime nature of **3a–d**, on the other hand, was confirmed by the additional singlet around δ 11.6 ppm and carbon signal significantly upfield around $\delta_{C=N}$ 154 ppm in their ^{1}H-NMR and ^{13}C-NMR spectra, respectively.

Scheme 1: $PdCl_2$-mediated *endo-dig* cyclization of **1a–d** and subsequent oximation of **2a–d**

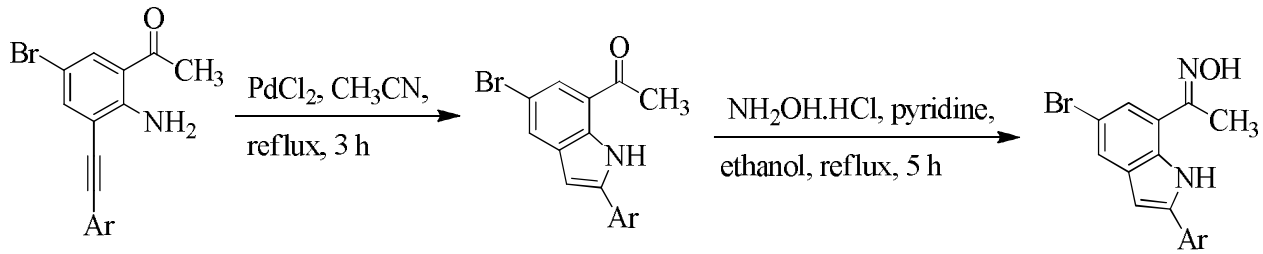

1a–d **3a–d** **2a–d**

Table 1: Percentage yields of compounds **2a–d** and **3a–d**

Compound	Ar	%Yield of 2	%Yield of 3
a	C_6H_5-	92	90
b	4-FC_6H_4-	84	87
c	3-ClC_6H_4-	85	82
d	4-MeOC_6H_4-	77	80

The oxime derivatives **3a–d** were, in turn, subjected to trifluoroacetic acid (TFA)-mediated Beckmann rearrangement in acetonitrile under reflux for 2 h to afford the corresponding 7-acetamido-2-aryl-5-bromoindoles **4a–d** (Scheme 2, Table 2). The proton NMR spectra of these amide derivatives revealed the presence of a singlet around δ 9.70 ppm corresponding to NH of the amide group. Formation of these compounds through an aryl carbon migration, on the other hand, was confirmed by a significant up-field shift of the methyl protons to around δ 2.18 ppm compared to those in the ^{1}H-NMR spectra of **2** (around δ 2.79 ppm) and **3** (around δ 2.30 ppm). Their carbonyl carbon resonates significantly up-field ($\delta_{C=O}$ 170 ppm) than that of the corresponding precursors **2** ($\delta_{C=O}$ 200 ppm) and more downfield than substrates **3** ($\delta_{C=N}$ 154 ppm).

Scheme 2: Beckmann rearrangement of **3a–d** to afford **4a–d**

Preprints (www.preprints.org) | NOT PEER-REVIEWED | Posted: 4 May 2018 doi:10.20944/preprints201805.0085.v1

Peer-reviewed version available at Pharmaceuticals 2018, 11, 59; doi:10.3390/ph11020059

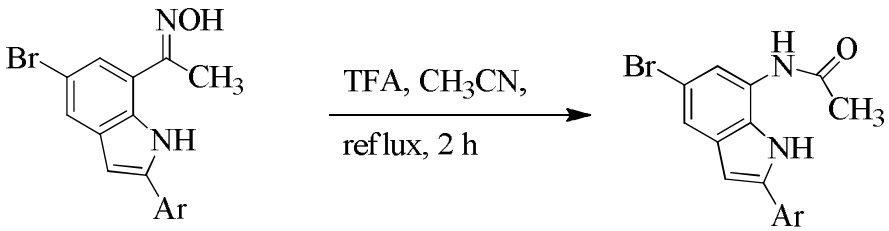

3a–d

4a–d

Table 2: Percentage yields of compounds **4a–d**

Compound	Ar	%Yield of 4
4a	C_6H_5-	81
4b	4-FC_6H_4-	76
4c	3-ClC_6H_4-	73
4d	4-$MeOC_6H_4$-	76

Friedel-Crafts C-3 trifluoroacetylation of the *N*-benzyl substituted 2-methyl-5-nitroindole [16], the *N*-unprotected 2-arylindoles [17], and their indole-chalcone derivatives [18] using trifluoroacetic anhydride (TFAA) has been found to circumvent competitive formation of the 1-acylated and/or the 1,3-diacylated products. A series of fluoromethyl indol-3-yl ketones has also been prepared via Friedel-Craft fluoroacetylation of indoles with fluorinated acetic acids (3 equiv.) in dichloroethane at 100 °C in the absence of catalyst or additive [19]. Compounds **2a–d** and **4a–d** were subjected to TFAA (1.2 equiv.) in THF under reflux for 5 h to afford the corresponding 7-acetyl **5a–d** and 7-acetamido substituted 5-bromo-3-trifluoroacetylindoles **5e–h** in moderate to high yields (Table 3, Scheme 3).

Scheme 3: Trifluoroacetylation of the 7-acetyl- **2a–d** and 7-acetamido-2-aryl-5-bromoindoles **4a–h**.

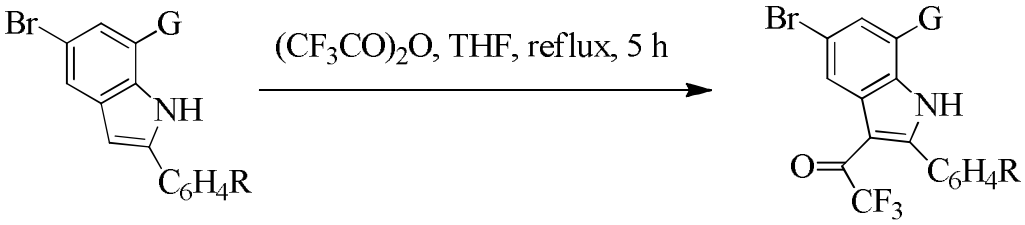

2a–d (G = -C(O)CH_3)

5a–d (G = -C(O)CH_3)

4a–d (G = -NHC(O)CH_3)

5e–h (G = -NHC(O)CH_3)

Table 3: Percentage yields of compounds **5a–h**

Compound	G	Ar	%Yield of 5
5a	-C(O)CH_3	C_6H_5-	92
5b	-C(O)CH_3	4-FC_6H_4-	84
5c	-C(O)CH_3	3-ClC_6H_4-	85
5d	-C(O)CH_3	4-$MeOC_6H_4$-	77

Preprints (www.preprints.org) | NOT PEER-REVIEWED | Posted: 4 May 2018 doi:10.20944/preprints201805.0085.v1

Peer-reviewed version available at Pharmaceuticals 2018, 11, 59; doi:10.3390/ph11020059

5e	-NHC(O)CH_3	C_6H_5-	84
5f	-NHC(O)CH_3	4-FC_6H_4-	78
5g	-NHC(O)CH_3	3-ClC_6H_4-	80
5h	-NHC(O)CH_3	4-MeOC_6H_4-	52

2.2 *Biological evaluation*

As a prelude to the 3-trifluoroacetyl–substituted 2-arylindole derivatives with potential anticancer properties, compounds **5a–h** were evaluated for antiproliferative properties *in vitro* against the human lung cancer (A549) and cervical cancer (HeLa) cell lines, which are the leading causes of death in males and females worldwide. The corresponding 3-unsubstituted 7-acetyl-2-aryl-5-bromoindole **2a–d** and 7-acetamido-2-aryl-5-bromoindole **4a–d** precursors were also included in the assays in order to correlate between both structural variations and cytotoxicity.

2.2.1 *In vitro* cytotoxicity studies of indole derivatives **2a–d**, **4a–d** and **5a–h**

The HeLa and A549 cancer cells were initially exposed to two concentrations of each test compound (10 μM and 100 μM) for 48 h with Melphalan, a well-known chemotherapeutic drug used as a positive control at the same concentrations (Tables 4 and 5). Acquisition was performed using the ImageXpress Micro XLS Widefield Microscope and the acquired images were analyzed using the MetaXpress software and Multi-Wavelength Cell Scoring Application Module (see Supplementary Information (Figure S2) for the corresponding cell viability percentages for each compound). The structure activity relationship (SAR) of these compounds has been evaluated with respect to the substitution patterns on the 2-phenyl ring, C-3 and C-7 positions. The acetyl derivatives **2a–d** were found to be generally inactive against the two cancer cell lines at both concentrations (Table 4). Replacement of the acetyl group with an acetamido moiety, on the other hand, resulted in modest activity against both cell lines for the 2-(4-fluorophenyl)- **4b**, 2-(3-chlorophenyl)- **4c** and 2-(4-methoxyphenyl)-substituted 7-acetamido-5-bromoindole **4d** (Table 4). The presence of the amide moiety on the fused benzo ring has previously been found to enhance the biological activity of indole-based compounds [6,10,12,20]. Lack of cytotoxicity against both cancer cell lines for the 2-phenyl substituted derivative **4a**, on the other hand, presumably reflects the importance of a lipophilic substituent (halogen or methoxy group) on the 2-phenyl ring of compounds **4b–d** on biological activity.

Table 4: IC_{50} values of compounds **2a–d** , **4a–d** and Melphalan against the A549 and HeLa cells

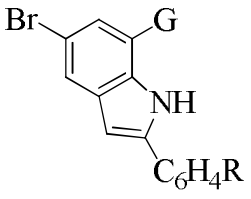

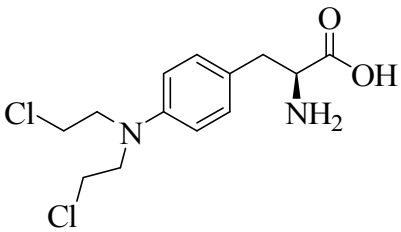

2a–d (G = -C(O)CH_3); **4a–d** (G = -NHC(O)CH_3) **Melphalan**

Preprints (www.preprints.org) | NOT PEER-REVIEWED | Posted: 4 May 2018 doi:10.20944/preprints201805.0085.v1

Peer-reviewed version available at Pharmaceuticals 2018, 11, 59; doi:10.3390/ph11020059

Compound	G	Ar	Cancer cells IC_{50} (μM) (A549)	HeLa
2a	-C(O)CH_3	C_6H_5-	>200	>200
2b	-C(O)CH_3	4-FC_6H_4-	>200	>200
2c	-C(O)CH_3	3-ClC_6H_4-	>200	>200
2d	-C(O)CH_3	4-MeOC_6H_4-	>200	>200
4a	-NHC(O)CH_3	C_6H_5-	>200	>200
4b	-NHC(O)CH_3	4-FC_6H_4-	116.2	122.4
4c	-NHC(O)CH_3	3-ClC_6H_4-	154.6	126.9
4d	-NHC(O)CH_3	4-MeOC_6H_4-	146.8	125.0
Melphalan			30.66	37.16

Diminished activity against both cell lines was observed for all the 2-aryl-5-bromoindoles **5a–d** bearing a combination of the 7-acetyl and 3-trifluoroacetyl groups (Table 5). A combination of a 7-acetamido and 3-trifluoroacetyl groups in compounds **5e–h**, on the other hand, resulted in increased cytotoxicity against both cancer cell lines and more so than the chemotherapeutic drug, Melphalan, used as a positive control at the same concentrations (see Supplementary Information (Figure S3) for the corresponding dose response curves). Within this series, the trend in IC_{50} values (Table 5) against the lung cancer (A549) cell line is as follows: **5g** (2.72 μM) > **5h** (3.26 μM) > **5f** (5.03 μM) > **5e** (9.94 μM) with the following trend in activity against the cervical cancer (HeLa) cells: **5f** (7.95 μM) > **5g** (8.74 μM) > **5h** (10.72 μM) > **5e** (12.89 μM). These preliminary cytotoxicity results suggest that a combination of the 7-acetamido and 3-trifluoroacetyl group is desirable for cytotoxicity of the 2-aryl-5-bromoindoles against both cancer cell lines. The slight antiproliferative activity observed for the corresponding C-3 unsubstituted 7-acetamido-5-bromoindoles **4a–d**, which significantly increased upon incorporation of a 3-trifluoroacetyl in derivatives **5e–h** further confirm the importance of a strong hydrogen bond acceptor at this position 3 of the indole framework to facilitate interaction with biological receptors in analogy with the literature precedents [9,10]. The strong electron-withdrawing effect of the trifluoromethyl group (-CF_3) has previously been found to generally increase the lipophilicity, metabolic stability and activity profile of indole derivatives compared to corresponding 3-unsubstituted [11] or 3-acetyl analogues [13]. The combined electron-withdrawing and hydrogen bonding effects of the trifluomethyl and carbonyl fragments of the 3-trifluoroacetyl group probably account for the observed increased cytotoxicity of compounds **5e–h**.

Table 5: IC_{50} values of compounds **5a–h** against A549 and HeLa cells

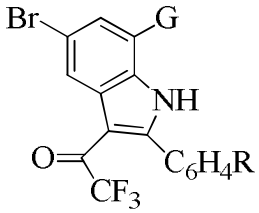

5a–d (G = -C(O)CH_3); **5e–h** (G = -NHC(O)CH_3)

	Cancer cells IC_{50} (μM)

Preprints (www.preprints.org) | NOT PEER-REVIEWED | Posted: 4 May 2018 doi:10.20944/preprints201805.0085.v1

Peer-reviewed version available at Pharmaceuticals 2018, 11, 59; doi:10.3390/ph11020059

Compound	G	Ar	(A549)	HeLa
5a	-C(O)CH_3	C_6H_5-	>200	>200
5b	-C(O)CH_3	4-FC_6H_4-	>200	>200
5c	-C(O)CH_3	3-ClC_6H_4-	>200	>200
5d	-C(O)CH_3	4-MeOC_6H_4-	>200	>200
5e	-NHC(O)CH_3	C_6H_5-	9.94	12.89
5f	-NHC(O)CH_3	4-FC_6H_4-	5.03	7.95
5g	-NHC(O)CH_3	3-ClC_6H_4-	2.72	8.74
5h	-NHC(O)CH_3	4-MeOC_6H_4-	3.26	10.72
Melphalan			30.66	37.16

In vitro studies indicated that indole derivatives such as indole-3-carbinol inhibit cell proliferation, caused cell cycle arrest at G1 phase and induced apoptosis [15]. Deregulation of apoptosis plays a significant role in the development of a variety of human pathologies including cancer [21]. Since cytotoxicity does not define a specific cellular death mechanism (necrosis or apoptosis), we took into consideration the pro-apoptotic properties of indole derivatives such as indole-3-carbinol [15] and selected compounds **4c** and **5g** as representative examples for further evaluation regarding the mechanism of action of the 3-trifluoroacetylated 2-arylindole derivatives **5e–h** in the A549 and HeLa cells.

2.2.2 Evaluation of cell death pathways

Several distinctive modes of cell death such as apoptosis, necrosis, autophagy and cornification exist and are characterized by differences in morphology and biochemical changes [22]. A major biochemical feature of apoptosis is the activation of caspases, which plays a central role in the morphological changes associated with apoptosis [23-25]. Caspase activation was determined using immunochemical methods and the antibodies against activated caspase 8 and caspase 3. Caspase 8 is an initiator caspase, which is first activated through a death signal suggesting a cellular response to an external signal for cell death. Activated caspase 8 can be used as a convenient indicator of involvement of the extrinsic death receptor pathway of apoptosis [26]. Executioner caspases including caspase 3 are, in turn, activated by the initiator caspases. This protein is either partially or totally responsible for the cleavage of many key proteins such as PARP, DNA protein kinases and retinoblastoma protein [27]. Figures 2 and 3 show the results of caspase activation analysis and it is evident that clear increases in the percentage of mean fluorescence intensity of the untreated control occurred when the HeLa and A549 cells were treated with **4c** and Melphalan. A decrease in percentage was noticed when HeLa cells were treated with **5g**, but the expected increase was evident in A549 cells. This was true for both activated caspase 8 and 3. A more distinct increase was evident with caspase 3 albeit less pronounced than that of **4c** and the increase was expected as caspase 3 is activated by initiator caspase including caspase 8, which is a later event in apoptosis. It is evident that **5g** induced apoptosis in a caspase-dependent manner in both cell lines and this effect is more pronounced for the A549 cells, which also showed increased sensitivity towards this compound in the cytotoxicity assays than the HeLa cells. Prolonged treatment of the cells with compounds **5e–h** for 48 h or more, for example, would probably result in significant effects. We also evaluated compound **5g** for potential to induce other key apoptotic biochemical features such as phosphatidylserine (PS) translocation, cell cycle arrest and mitochondrial membrane depolarization.

Preprints (www.preprints.org) | NOT PEER-REVIEWED | Posted: 4 May 2018 doi:10.20944/preprints201805.0085.v1

Peer-reviewed version available at Pharmaceuticals 2018, 11, 59; doi:10.3390/ph11020059

However, the compound failed to induce PS translocation, cell cycle arrest and mitochondrial membrane depolarization in both cell lines after 24 h (data not included).

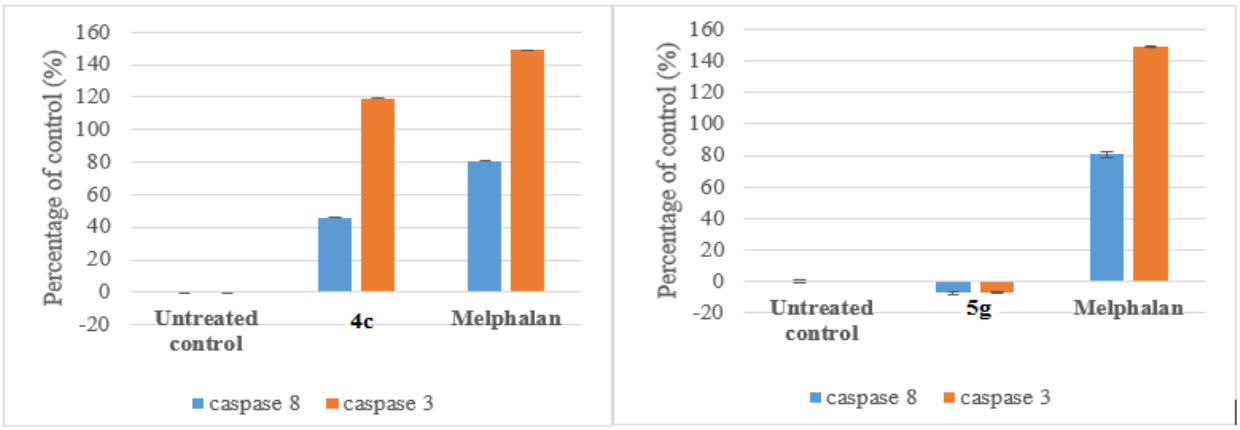

Figure 2: Caspase 8 and 3 activation as indicated by % changes in the mean integrated fluorescence intensity of the untreated control using HeLa cells after 24 h of exposure to compounds **4c** and **5g** (IC_{50} values) using Melphalan as a positive control. Bar graph represents the average of one individual experiment performed in quadruplicate. SD is represented as error bars.

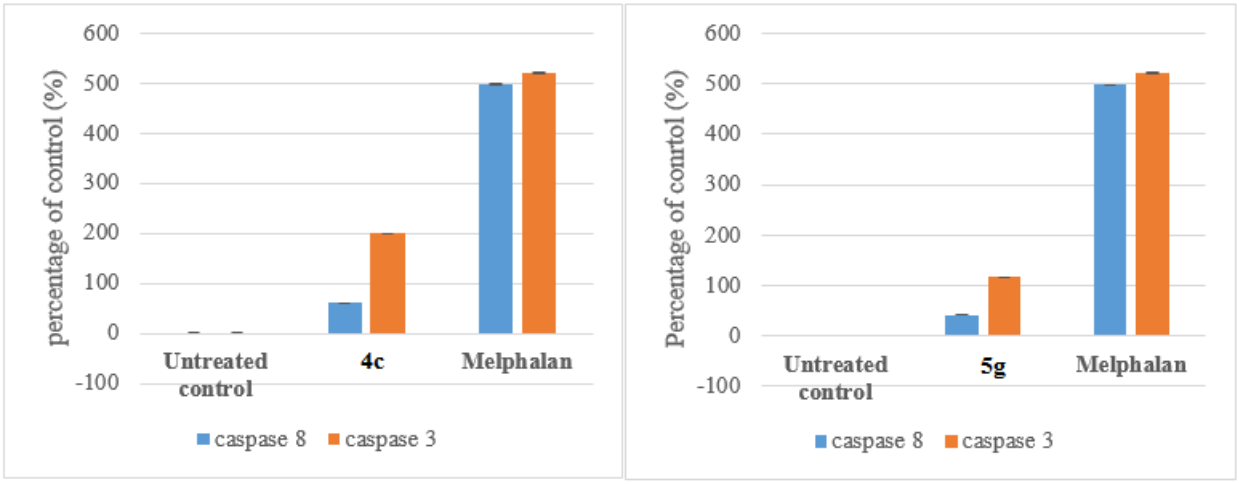

Figure 3: Caspase 8 and 3 activation as indicated by % changes in the mean integrated fluorescence intensity of the untreated control using A549 cells after 24 h of exposure to **4c** and **5g** (IC_{50} values) using Melphalan as a positive control. Bar graph represents the average of one individual experiment performed in quadruplicate. SD is represented as error bars.

Recourse to the literature revealed that a series of analogous indole-bearing combretastatin derivatives prepared by condensing indole-3-acetic acid with aldehydes prevent tubulin polymerization as confirmed by immunofluorescence confocal microscopy [28]. Molecular docking revealed that the compounds bind to the colchicine binding site which is situated at α and β interface of tubulin [28]. This literature precedent encouraged us to evaluate the 3-trifluoroacetyl substituted derivatives **5e–h** for potential to inhibit tubulin polymerization.

2.4 *Effect of compounds **5e–h** on tubulin polymerization*

In order to determine if the antiproliferative activity of compounds **5e–h** was related to their capacity to destabilize tubulin, we evaluated them in a tubulin polymerization assay tubulin polymerization using

Preprints (www.preprints.org) | NOT PEER-REVIEWED | Posted: 4 May 2018 doi:10.20944/preprints201805.0085.v1

Peer-reviewed version available at Pharmaceuticals 2018, 11, 59; doi:10.3390/ph11020059

colchicine and indole-3-carbinol as reference standards. Kinetics of inhibition of tubulin polymerization of compounds **5e–h** at 0.25 μM against colchicine and indole-3-carbinol as reference standards (Figure 4) revealed that these compounds significantly interfere with tubulin polymerization by lowering the rate of microtubule assembly. The IC_{50} values for compounds **5a–e** and the corresponding reference standards (Table 5) were obtained at the following concentrations: 0.1, 1.0 and 10 μM. These results are in agreement with the antiproliferative activity in the cell culture.

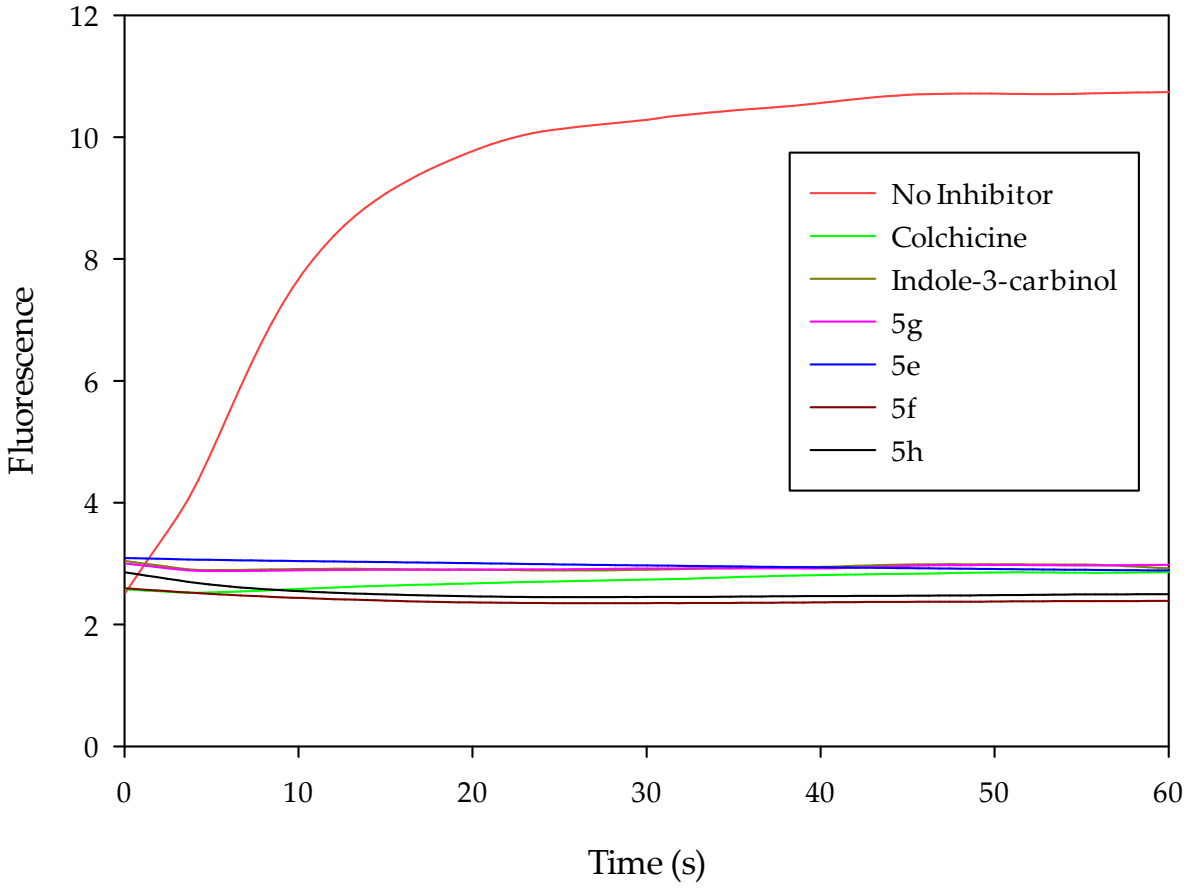

Figure 4: Kinetics of inhibition of tubulin polymerization by **5e–h** at 0.25 μM against colchicine (green) and indole-3-carbinol (yellow) and in the absence of an inhibitor (red). Fluorescence at 450 nm was measured every three seconds over a period of 1 h at 37 °C.

Table 6: IC_{50} values of **5e–h** against tubulin using indol-3-carbinol and colchicine as positive controls

Compound	Tubulin IC_{50} (μM)
5e	3.18×10^{-5}
5f	3.28×10^{-7}
5g	2.42×10^{-5}
5h	4.86×10^{-6}
Indol-3-carbinol	9.76×10^{-5}
Colchicine	9.88×10^{-5}

Preprints (www.preprints.org) | NOT PEER-REVIEWED | Posted: 4 May 2018 doi:10.20944/preprints201805.0085.v1

Peer-reviewed version available at Pharmaceuticals 2018, 11, 59; doi:10.3390/ph11020059

We attribute increased cytotoxicity and inhibition of tubulin polymerization of compounds **5e–h** to strong interaction with the active site of the receptor, which may involve strong hydrogen bond interactions between the trifluoroacetyl and the acetamido groups of the ligands with the receptor's protein residues. In order to prove this assumption and further guide structure activity relationship (SAR) studies, molecular docking was performed on the most active compound **5g** into the colchicine-binding site of tubulin.

*2.5 Molecular docking studies of **2a**, **4a** and **5g** into tubulin*

To help us understand the anticancer activity of the 3-trifluoroacetyl indole derivatives **5e–h** and further rationalize SAR, we docked **5g** and the corresponding parent compounds **2a** and **4a** into tubulin (Figure 5). A crystal structure of tubulin was obtained from the protein data bank (PDB ID: 1TUB). Compounds **2a**, **4a** and **5g** docked to tubulin between the two subunits of the heterodimer (Figure 5).

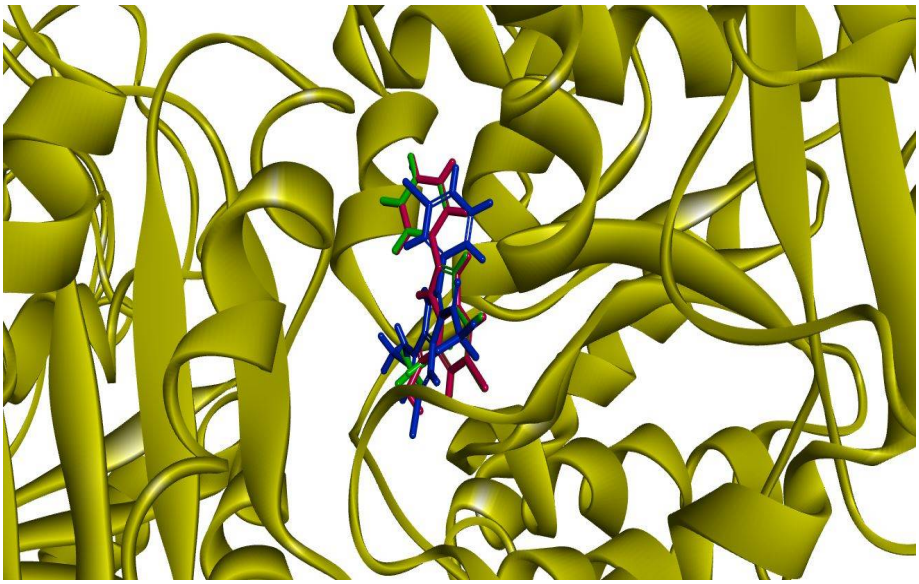

Figure 5: Compounds **2a** (green), **4a** (pink) and **5g** (blue) docked at the dimer interface of a tubulin heterodimer (PDB code: 1TUB) with chain coloured yellow.

Several binding interactions involving pi-alkyl, amide-pi stacked and alkyl interactions were observed between the compounds and the active site residues, for example, Ala12, Val177, Val182, Leu248, Ile171 and Tyr224 (Figure 6). There is no hydrogen bonding between the acetyl group of **2a** and any of the protein residues. Molecular docking and the results of cytotoxicity against both cell lines seem to suggest that the presence of an acetyl group at the 7-position of the fused benzo ring is not desirable for cytotoxicity. However, the presence of a carbonyl (formyl or acetyl) group was previously found to enhance the antiproliferative properties of the indoles when attached to the C-3 position [9]. Molecular docking, on the other hand, revealed the presence of a hydrogen bond between the amide functionality of **4a** and the protein residue Ala12. The propensity of the amide moiety for hydrogen bonding has previously been found to play an important role in the interaction of bioactive compounds with the receptors [29], which probably accounts for the observed slight cytotoxicity of compounds **4b–d** against the two cancer cell lines when compared to **2a–d**. Compound **5g** gets stabilized in the colchicine-binding site of tubulin by the hydrophobic and hydrogen bond interactions. The presence of the trifluoroacetyl group in **5g** resulted in hydrogen bonding between the carbonyl group and fluorine atoms with the protein residue Asn206. Additional hydrogen bond interaction is observed between the acetamido group

Preprints (www.preprints.org) | NOT PEER-REVIEWED | Posted: 4 May 2018 doi:10.20944/preprints201805.0085.v1

Peer-reviewed version available at Pharmaceuticals 2018, 11, 59; doi:10.3390/ph11020059

of compound **5g** and Asn101 with π-π stacking interaction between the protein residue Tyr224 and the 3-chlorophenyl group. These interactions probably help to stabilize the binding of compounds **5a–h** in the colchicine-binding domain of α,β-tubulin interface. A 3-trifluoroacetyl moiety in the 7-acetamido-2-aryl-5-bromoindoles **5e–h** in our view enhances the binding of these compounds to tubulin in the colchicine-binding domain of α,β-tubulin interface. Such binding would probably affect the microtubule changes that take place in cells during cell division and hence lead to cell death.

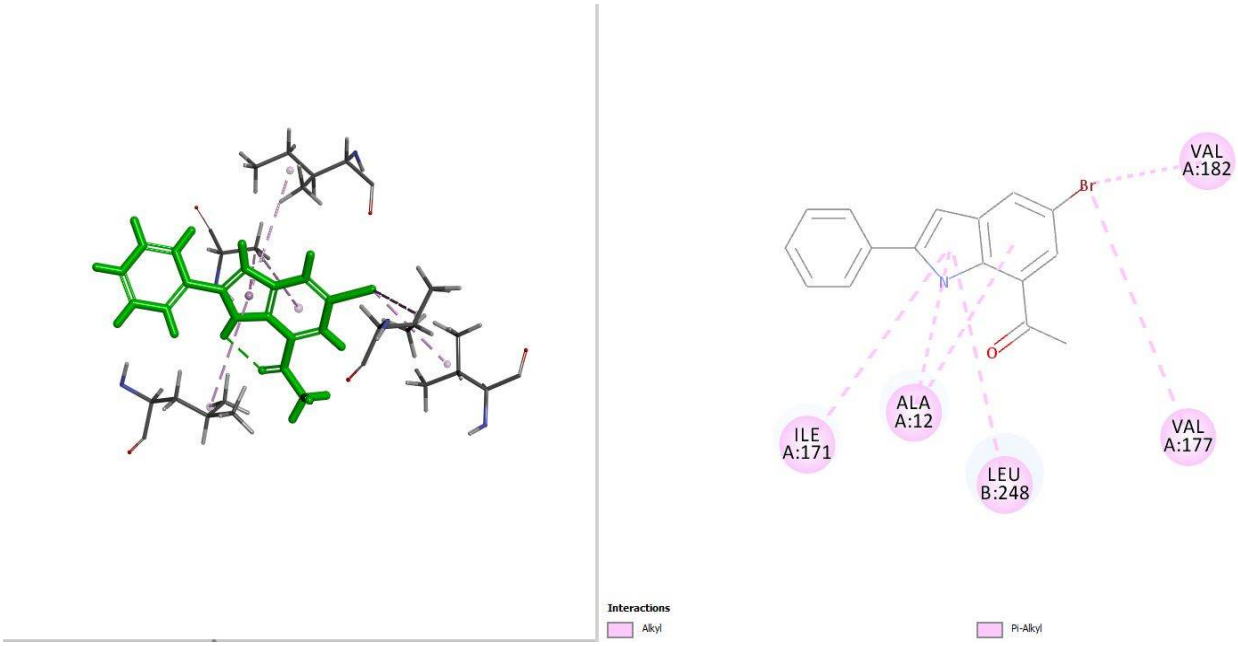

1-(5-bromo-2-phenyl-1*H*-indol-7-yl)ethanone (**2a**)

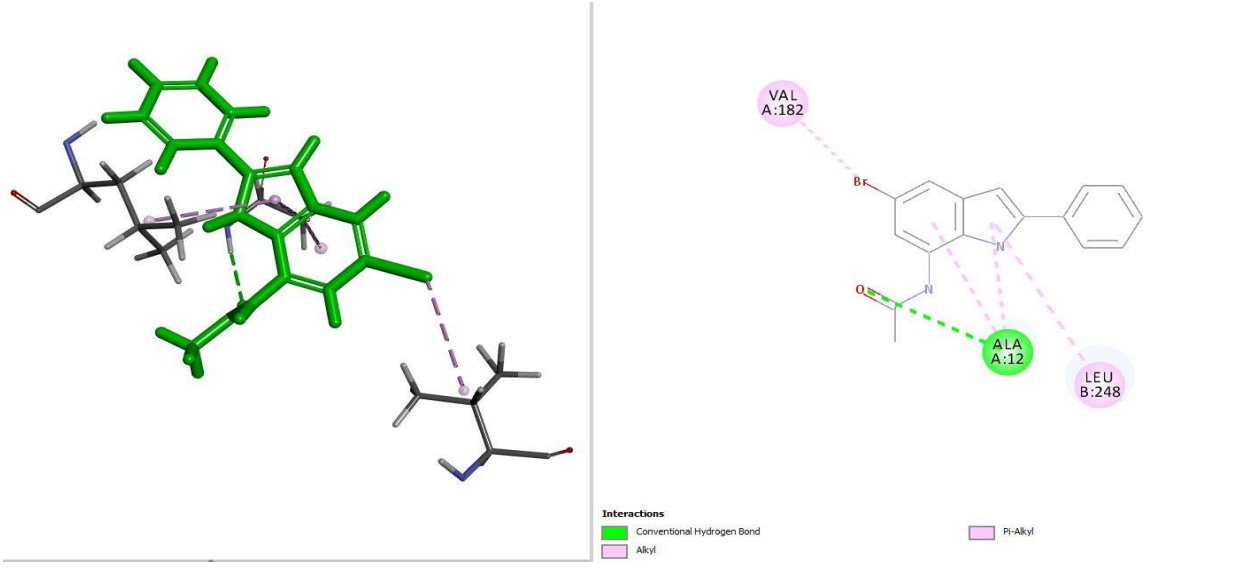

N-(5-bromo-2-phenyl-1*H*-indol-7-yl)acetamide (**4a**)

Preprints (www.preprints.org) | NOT PEER-REVIEWED | Posted: 4 May 2018 doi:10.20944/preprints201805.0085.v1

Peer-reviewed version available at Pharmaceuticals 2018, 11, 59; doi:10.3390/ph11020059

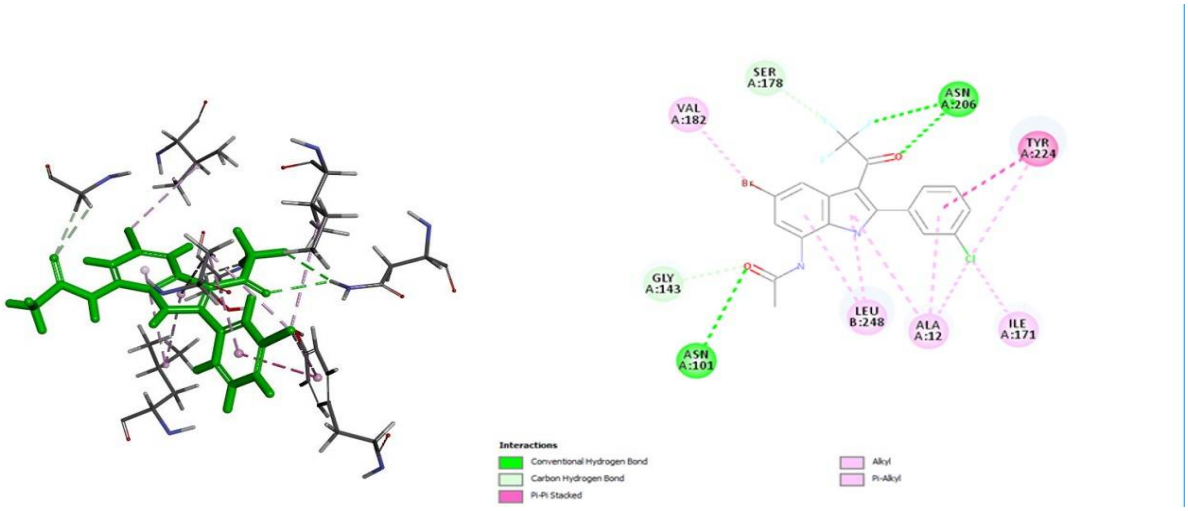

N-(5-bromo-3-(4-chlorophenyl)-3-(2,2,2-trifluroacetyl)-1*H*-indol-7-yl)acetamide (**5g**)

Figure 6: 2D interaction diagrams for the binding of tubulin (PDB code 1TUB) with **2a**, **4a** and **5g**. Residues are annotated with their 3-letter amino acid code and interactions listed below the diagram.

3. Materials and Methods

3.1 General

Melting points were recorded on a Thermocouple digital melting point apparatus and are uncorrected. IR spectra were recorded as powders using a Bruker VERTEX 70 FT-IR Spectrometer (Bruker Optics, Billerica, MA, USA) with a diamond ATR (attenuated total reflectance) accessory by using the thin-film method. For column chromatography, Merck kieselgel 60 (0.063–0.200 mm) (Merck KGaA, Frankfurt, Germany) was used as stationary phase. NMR spectra were obtained as DMSO-d_6 solutions using Agilent 300 MHz NMR (Agilent Technologies, Oxford, UK) spectrometer and the chemical shifts are quoted relative to the TMS peak. Low- and high-resolution mass spectra were recorded at an ionization potential of 70 eV using Waters Synapt G2 Quadrupole Time-of-flight mass spectrometer (Waters Corp., Milford, MA, USA) at the University of Stellenbosch Central Analytical Facility. The synthesis and characterization of compounds **1a–d** [14] have been described before.

*3.2 Typical procedure for the $PdCl_2$-mediated heteroannulation of **1a–d***

A stirred mixture of **1** (1 equivalent) and $PdCl_2$ (0.2 equivalent) in acetonitrile (15 mL/mmol of **1**) was heated at 80 °C under argon atmosphere for 3 h. The mixture was evaporated to dryness and the residue was dissolved in chloroform. The organic solvent was washed with brine and dried over $MgSO_4$. The salt was filtered off and the solvent was evaporated under reduced pressure. The residue was purified by column chromatography on a silica gel using 10% EtOAc-hexane as eluent to afford **2** as a solid. Compounds **2a–d** were prepared in this fashion.

1-(5-Bromo-2-phenyl-1H-indol-7-yl)ethanone (**2a**). A mixture of **1a** (1.00 g, 3.18 mmol) and $PdCl_2$ (0.11 g, 0.64 mmol) in acetonitrile (50 mL) afforded **2a** as a solid (0.92 g, 92%), R_f 0.36, mp. 139–142 °C; ν_{max} (ATR) 550, 596, 671, 750, 849, 961, 1043, 1163, 1230, 1251, 1322, 1360, 1448, 1490, 1516, 1595, 1650, 3436 cm^{-1}; ^{1}H-NMR (DMSO-d_6) 2.71 (3H, s, CH_3), 6.98 (1H, s, 3-H), 7.38 (1H, t, J = 7.5 Hz, 4'-H), 7.47 (2H, t, J = 7.5 Hz, 3',5'-H), 7.89 (2H, d, J = 7.5 Hz, 2',6'-H), 7.94 (1H, d, J = 1.2 Hz, 4-H), 8.05 (1H, d, J = 1.2 Hz, 6-H), 11.14 (1H, s, NH); ^{13}C-NMR (DMSO-d_6) 27.6, 99.5, 111.7, 122.1, 126.4, 127.4, 128.6, 128.9, 129.4, 131.3, 132.6, 134.0, 141.3, 199.2;

Preprints (www.preprints.org) | NOT PEER-REVIEWED | Posted: 4 May 2018 doi:10.20944/preprints201805.0085.v1

Peer-reviewed version available at Pharmaceuticals 2018, 11, 59; doi:10.3390/ph11020059

m/z 314 (100, M+H); HRMS (ES): found 314.0191. $C_{16}H_{13}NO^{79}Br^+$ requires 314.0181. *Anal* calcd for $C_{16}H_{12}NOBr$: C, 61.17; H, 3.85; N, 4.46. Found: C, 61.02; H, 3.79; N, 4.52.

1-[5-Bromo-2-(4-fluorophenyl)-1H-indol-7-yl]ethanone (**2b**). A mixture of **1b** (1.00 g, 3.01 mmol) and $PdCl_2$ (0.11 g, 0.60 mmol) in acetonitrile (50 mL) afforded **2b** as a solid (0.84 g, 84%), R_f 0.35, mp. 171–173 °C; ν_{max} (ATR) 549, 749, 786, 835, 925, 1006, 1043, 1162, 1231, 1251, 1321, 1360, 1449, 1491, 1578, 1595, 1650, 3436 cm^{-1}; ^{1}H-NMR (DMSO-d_6) 2.69 (3H, s, CH_3), 6.91 (1H, s, 3-H), 7.29 (2H, t, J = 8.7 Hz, 3',5'-H), 7.91–7.95 (3H, m, 4-H and 2',6'-H), 8.01 (1H, d, J = 1.2 Hz, 6-H), 11.19 (1H, s, NH); ^{13}C-NMR (DMSO-d_6) 27.6, 99.4, 111.7, 116.2 (d, $^2J_{CF}$ = 21.8 Hz), 122.2, 127.3, 128.0 (d, $^4J_{CF}$ = 3.5 Hz), 128.5, 128.8 (d, $^3J_{CF}$ = 8.0 Hz), 132.5, 134.0, 140.5, 162.2 (d, $^1J_{CF}$ = 243.9 Hz), 199.1; m/z 332 (100, M+H); HRMS (ES) found 332.0090. $C_{16}H_{12}NO^{79}FBr^+$ requires 332.0086. *Anal* calcd for $C_{16}H_{11}NOFBr$: C, 57.85; H, 3.34; N, 4.22. Found: C, 57.79; H, 3.30; N, 4.12.

1-[5-Bromo-2-(3-chlorophenyl)-1H-indol-7-yl]ethanone (**2c**). A mixture of **1c** (1.00 g, 2.87 mmol) and $PdCl_2$ (0.10 g, 0.57 mmol) in acetonitrile (50 mL) afforded **2c** as a solid (0.77 g, 77%), R_f 0.34, mp. 140–143 °C; ν_{max} (ATR) 452, 542, 572, 673, 751, 785, 852, 878, 969, 1052, 1082, 1164, 1252, 1323, 1357, 1452, 1590, 1653, 3424 cm^{-1}; ^{1}H-NMR (DMSO-d_6) 2.69 (3H, s, CH_3), 7.04 (1H, s, 3-H), 7.38–7.49 (2H, m, 4',5'-H), 7.82–7.86 (1H, d, J = 8.7 Hz, 6'-H), 7.93 (1H, d, J = 1.2 Hz, 4-H), 8.03–8.04 (2H, m, 2′-H and 6-H), 11.33 (1H, s, NH); ^{13}C-NMR (DMSO-d_6) 27.6, 100.7, 111.8, 122.4, 125.2, 126.2, 127.8, 128.4, 128.7, 131.0, 132.3, 133.4, 134.0, 134.1, 139.8, 198.9; m/z 348 (100, M+H); HRMS (ES): found 347.9779. $C_{16}H_{12}NO^{35}Cl^{79}Br^+$ requires 347.9791. *Anal* calcd for $C_{16}H_{11}NOClBr$: C, 55.12; H, 3.18; N, 4.02. Found: C, 55.10; H, 3.33; N, 3.89.

1-[5-Bromo-2-(4-methoxyphenyl)-1*H*-indol-7-yl]ethanone (**2d**). A mixture of **1d** (1.00 g, 2.91 mmol) and $PdCl_2$ (0.10 g, 0.58 mmol) in acetonitrile (50 mL) afforded **2d** as a solid (0.85 g, 85%), R_f = 0.27, mp. 140–142 °C; ν_{max} (ATR) 550, 589, 749, 825, 925, 1028, 1162, 1181, 1253, 1290, 1321, 1361, 1451, 1497, 1578, 1654, 3433 cm^{-1}; ^{1}H-NMR (300 MHz, DMSO-d_6) 2.69 (3H, s, CH_3), 3.80 (3H, s, OCH_3), 6.86 (1H, s, 3-H), 7.03 (2H, d, J = 8.7 Hz, 3',5'-H), 7.84 (2H, d, J 8.7 Hz, 2',6'-H), 7.90 (1H, d, J = 1.2 Hz, 4-H), 8.01 (1H, d, J = 1.2 Hz, 6-H), 11.06 (1H, s, NH); ^{13}C-NMR (DMSO-d_6) 27.6, 55.7, 98.2, 111.6, 114.8, 121.9, 123.8, 126.8, 127.9, 128.2, 132.8, 133.9, 141.5, 160.0, 199.3; m/z 344 (100, M+H); HRMS (ES) found 344.0289. $C_{17}H_{15}NO_2{}^{79}Br^+$ requires 344.0286. *Anal* calcd for $C_{17}H_{14}NO_2Br$: C, 59.32; H, 4.10; N, 4.07. Found: C, 59.32; H, 3.87; N, 4.10.

3.3 Typical procedure for the synthesis of oxime derivatives **3a–d** *from* **2a–d**

A stirred mixture of **2** (1 equivalent) and hydroxylamine hydrochloride (1.5 equivalent) and pyridine (1.5 equivalent) in ethanol (20 mL/mmol of **2**) was heated at 80 °C for 5 h. The mixture was cooled to room temperature and quenched with an ice-cold water. The product was extracted into chloroform and the combined organic phases were washed with water and dried over anhydrous $MgSO_4$. The salt was filtered off and the solvent was evaporated under reduced pressure. The residue was purified by column chromatography on silica gel using 20% EtOAc-hexane as an eluent to afford the oxime derivative **3** as a solid. Products **3a–d** were prepared in this fashion:

1-(5-Bromo-2-phenyl-1H-indol-7-yl)ethanone oxime (**3a**). A mixture of **2a** (0.30 g, 0.95 mmol), hydroxylamine hydrochloride (0.10 g, 1.43 mmol) and pyridine (0.11 g, 1.43 mmol) in ethanol (20 mL) afforded **3a** as a solid (0.28 g, 90%), R_f = 0.69, mp. 198–200 °C; ν_{max} (ATR) 524, 542, 634, 679, 734, 763, 839, 989, 1093, 1172, 1261, 1298, 1331, 1368, 1448, 3269, 3438 cm^{-1}; ^{1}H-NMR (DMSO-d_6) 2.30 (3H, s, CH_3), 6.96 (1H, s, 3-H), 7.37 (1H, t, J = 7.5 Hz, 4'-H), 746–7.52 (3H, m, 6-H and 3',5'-H), 7.78–7.81 (3H, m, 4-H and 2',6'-H), 10.94 (1H, s, NH), 11.56 (1H, s, OH); ^{13}C-NMR (DMSO-d_6) 11.2, 99.3, 112.4, 121.7, 123.4, 123.8, 125.5, 128.7, 129.6, 131.3, 131.5, 132.5, 139.2, 154.1; m/z 329 (100, M+H); HRMS (ES): found 329.0276. $C_{16}H_{14}N_2O^{79}Br^+$ requires 329.0290.

Preprints (www.preprints.org) | NOT PEER-REVIEWED | Posted: 4 May 2018 doi:10.20944/preprints201805.0085.v1

Peer-reviewed version available at Pharmaceuticals 2018, 11, 59; doi:10.3390/ph11020059

1-(5-Bromo-2-(4-fluorophenyl)-1H-indol-7-yl)ethanone oxime (**3b**). A mixture of **2b** (0.30 g, 0.90 mmol), hydroxylamine hydrochloride (0.09 g, 1.35 mmol) and pyridine (0.11 g, 1.35 mmol) in ethanol (20 mL) afforded **3b** as a solid (0.27 g, 87%), R_f = 0.64, mp. 213–216 °C; ν_{max} (ATR) 530, 595, 651, 680, 744, 764, 828, 846, 912, 984, 1091, 1159, 1230, 1332, 1366, 1428, 1464, 1501, 3258, 3432 cm^{-1}; ^{1}H-NMR (DMSO-d_6) 2.30 (3H, s, CH_3), 6.93 (1H, s, 3-H), 7.34 (2H, t, J = 8.7 Hz, 3',5'-H), 7.45 (1H, d, J = 1.2 Hz, 6-H), 7.77 (1H, d, J = 1.2 Hz, 4-H), 7.84–7.87 (2H, dd, J = 5.4 and 8.7 Hz, 2',6'-H), 10.92 (1H, s, NH), 11.56 (1H, s, OH); ^{13}C-NMR (DMSO-d_6) 11.3, 99.3, 112.5, 116.5 (d, $^2J_{CF}$ = 21.8 Hz), 121.8, 123.4, 123.7, 127.7 (d, $^3J_{CF}$ = 9.1 Hz), 128.3 (d, $^4J_{CF}$ = 3.5 Hz), 131.3, 132.5, 138.4, 154.0, 162.4 (d, $^1J_{CF}$ = 243.9 Hz); m/z 347 (100, M+H); HRMS (ES): found 347.0179. $C_{16}H_{13}N_2OF^{79}Br^+$ requires 347.0195.

1-(5-Bromo-2-(3-chlorophenyl)-1H-indol-7-yl)ethanone oxime (**3c**). A mixture of **2c** (0.30 g, 0.86 mmol), hydroxylamine hydrochloride (0.09 g, 1.29 mmol) and pyridine (0.10 g, 1.29 mmol) in ethanol (20 mL) afforded **3c** as a solid (0.26 g, 82%), R_f = 0.63, mp. 204–206 °C; ν_{max} (ATR) 454, 532, 631, 673, 742, 784, 847, 876, 947, 985, 1094. 1167, 1268, 1268, 1296, 1334, 1368, 1421, 1463, 3203, 3392 cm^{-1}; ^{1}H-NMR (DMSO-d_6) 2.32 (3H, s, CH_3), 7.09 (1H, s, 3-H), 7.44–7.55 (3H, m, 6-H and 4',5'-H), 7.78–7.81 (2H , m, 4-H and 6'-H), 7.92 (1H, s Hz, 2'-H), 11.02 (1H, s, NH), 11.60 (1H, s, OH); ^{13}C-NMR (75 MHz, DMSO-d_6) 11.5, 100.5, 112.6, 122.1, 123.8, 123.9, 124.2, 125.1, 128.3, 131.1, 131.4, 132.7, 133.4, 134.4, 137.7, 153.8; m/z 362 (100, M+H); HRMS (ES): found 362.9893. $C_{16}H_{13}N_2O^{35}Cl^{79}Br^+$ requires 362.9900.

1-(5-Bromo-2-(4-methoxyphenyl)-1H-indol-7-yl)ethanone oxime (**3d**). A mixture of **2d** (0.30 g, 0.87 mmol), hydroxylamine hydrochloride (0.09 g, 1.31 mmol) and pyridine (0.10 g, 1.31 mmol) in ethanol (20 mL) afforded **3d** as a solid (0.25 g, 80%), R_f = 0.45, mp. 202–204 °C; ν_{max} (ATR) 521, 585, 612, 653, 671, 755, 796, 826, 984, 1017, 1172, 1185, 1246, 1323, 1372, 1439, 1460, 1497, 3372, 3518 cm^{-1}; ^{1}H-NMR (DMSO-d_6) 2.30 (3H, s, CH_3), 3.80 (3H, s, OCH_3), 6.80 (1H, s, 3-H), 7.04 (2H, d, J = 8.7 Hz, 3',5'-H), 7.42 (1H, d, J = 1.2 Hz, 6-H), 7.70 (3H, m, 4-H and 2',6'-H), 10.84 (1H, s, NH), 11.57 (1H, s, OH); ^{13}C-NMR (DMSO-d_6) 11.3, 55.7, 98.0, 112.3, 115.0, 121.4, 122.9, 123.4, 124.2, 126.9, 131.6, 132.2, 139.4, 154.2, 159.8; m/z 359 (100, M+H); HRMS (ES): found 359.0293. $C_{17}H_{16}N_2O_2{}^{79}Br^+$ requires 359.0395.

3.4 Typical procedure for the Beckmann rearrangement of **3a–d**

A stirred mixture of **3** (1 equiv.) and TFA (1.2 equiv.) in acetonitrile (10 mL/ mmol of **3**) was heated at 80 °C for 2 h. The mixture was cooled to room temperature and quenched with ice-cold water. The product was extracted with chloroform (3 x 20 mL) and the combined organic layer was dried over anhydrous $MgSO_4$. The salt was filtered off and the solvent was evaporated under reduced pressure. The residue was purified by column chromatography on a silica gel using 60% EtOAc-hexane as an eluent to afford **4**. The following compounds were prepared in this fashion:

N-(5-Bromo-2-phenyl-1H-indol-7-yl)acetamide (**4a**). A mixture of **3a** (0.20 g, 0.61 mmol) and TFA (0.08 g, 0.73 mmol) in acetonitrile (15 mL) afforded **4a** as solid (0.16 g, 81%), R_f = 0.56, mp. 243–244 °C; ν_{max} (ATR) 518, 562, 600, 688, 740, 760, 842, 998, 1184, 1273, 1315, 1404, 1425, 1455, 1530, 1623, 1651, 3267, 3319 cm^{-1}; ^{1}H-NMR (DMSO-d_6) 2.19 (3H, s, CH_3), 6.88 (1H, s, 3-H), 7.38 (1H, t, J = 7.5 Hz, 4'-H), 7.46–7.52 (3H, m, 4-H and 3',5'-H), 7.82 (2H, d, J = 7.5 Hz, 2',6'-H), 7.88 (1H, d, J = 1.2 Hz, 6-H), 9.76 (1H, s, NH), 11.28 (1H, s, NH); ^{13}C-NMR (DMSO-d_6) 24.5, 99.5, 112.1, 115.5, 118.2, 125.5, 125.7, 127.3, 128.5, 129.5, 131.6, 131.9, 139.0, 169.1; m/z 329 (100, M+H); HRMS (ES): found 329.0265. $C_{16}H_{14}N_2O^{79}Br^+$ requires 329.0289. *Anal* calcd for $C_{16}H_{13}N_2OBr$: C, 58.38; H, 3.98; N, 8.51. Found: C, 58.24; H, 3.9q; N, 8.47.

N-[5-Bromo-2-(4-fluorophenyl)-1H-indol-7-yl]acetamide (**4b**). A mixture of **3b** (0.20 g, 0.58 mmol) and TFA (0.08 g, 0.69 mmol) in acetonitrile (15 mL) afforded **4b** as solid (0.14 g, 76%); R_f = 0.53, mp. 263–265 °C;

Preprints (www.preprints.org) | NOT PEER-REVIEWED | Posted: 4 May 2018 doi:10.20944/preprints201805.0085.v1

Peer-reviewed version available at Pharmaceuticals 2018, 11, 59; doi:10.3390/ph11020059

ν_{max} (ATR) 519, 576, 695, 744, 780, 837, 1000, 1163, 1231, 1274, 1318, 1438, 1474, 1502, 1542, 1624, 1654, 3267, 3355 cm^{-1}; ^{1}H-NMR (DMSO-d_6) 2.17 (3H, s, CH_3), 6.84 (1H, s, 3-H), 7.34 (2H, t, J = 8.7 Hz, 3',5'-H), 7.44 (1H, d, J = 1.2 Hz, 4-H), 7.82–7.86 (3H, m, 6-H and 2',6'-H), 9.71 (1H, s, NH), 11.23 (1H, s, NH); ^{13}C-NMR (DMSO-d_6) 24.5, 99.4, 112.2, 115.7, 116.5 (d, $^2J_{CF}$ = 21.8 Hz), 118.3, 125.4, 127.5, 127.8 (d, $^3J_{CF}$ = 8.0 Hz), 128.6 (d, $^4J_{CF}$ = 3.4 Hz), 131.5, 138.1, 162.3 (d, $^1J_{CF}$ = 243.9 Hz), 169.1; m/z 347 (100, M+H); HRMS (ES): found 347.0168. $C_{16}H_{13}N_2OF^{79}Br^+$ requires 347.0195. *Anal* calcd for $C_{16}H_{12}N_2OFBr$: C, 55.35; H, 3.48; N, 8.07. Found: C, 55.22; H, 3.39; N, 7.89.

N-(5-Bromo-2-(3-chlorophenyl)-1H-indol-7-yl)acetamide (**4c**). A mixture of **3c** (0.30 g, 0.55 mmol) and TFA (0.08 g, 0.66 mmol) in acetonitrile (15 mL) afforded **4c** as solid (0.15 g, 73%), R_f = 0.54, mp. 261–263 °C; ν_{max} (ATR) 562, 598, 668, 680, 751, 775, 846, 1010, 1095, 1277, 1317, 1445, 1462, 1538, 1573, 1622, 1650, 3268, 3397 cm^{-1}; ^{1}H-NMR (DMSO-d_6) 2.18 (3H, s, CH_3), 6.97 (1H, s, 3-H), 7.38–7.53 (3H, m, 4-H and 4',5'-H), 7.77 (1H, d. J = 8.7 Hz, 6'-H), 7.87–7.90 (2H, m, 6-H and 2'-H), 9.70 (1H, s, NH), 11.28 (1H, s, NH); ^{13}C-NMR (DMSO-d_6) 24.6, 100.6, 112.3, 116.2, 118.5, 124.4, 125.0, 125.5, 127.8, 128.1, 131.3, 131.4, 134.0, 134.4, 137.3, 169.1; m/z 363 (100, M+H); HRMS (ES): found 362.9890. $C_{16}H_{13}N_2O^{35}Cl^{79}Br^+$ requires 362.9900. *Anal* calcd for $C_{16}H_{12}N_2OClBr$: C, 52.85; H, 3.33; N, 7.70. Found: C, 52.78; H, 3.41; N, 7.59.

N-[5-Bromo-2-(4-methoxyphenyl)-1H-indol-7-yl]acetamide (**4d**). A mixture of **3d** (0.30 g, 0.56 mmol) and TFA (0.08 g, 0.67 mmol) in acetonitrile (15 mL) afforded **4d** as solid (0.16 g, 76%), R_f = 0.36, mp. 226–228 °C; ν_{max} (ATR) 559, 584, 694 786, 834, 1021, 1179, 1244, 1320, 1398, 1439, 1500, 1612, 1658, 3300, 3403 cm^{-1}; ^{1}H-NMR (DMSO-d_6) 2.18 (3H, s, CH_3), 3.80 (3H, s, OCH_3), 6.74 (1H, s, 3-H), 7.06 (2H, d, J = 8.7 Hz, 3',5'-H), 7.41 (1H, d, J = 1.2 Hz, 4-H), 7.74 (2H, d, J = 8.7 Hz, 2',6'-H), 7.83 (1H, d, J = 1.2 Hz, 6-H), 9.71 (1H, s, NH), 11.14 (1H, s, NH); ^{13}C-NMR (DMSO-d_6) 24.6, 55.7, 98.2, 112.0, 114.9 (2 x C), 115.1, 117.9, 124.5, 125.2, 127.1, 131.8, 139.1, 159.7, 169.1; m/z 359 (100, M+H); HRMS (ES): found 359.0393. $C_{17}H_{16}N_2O_2^{79}Br^+$ requires 359.0395. *Anal* calcd for $C_{17}H_{15}N_2O_2Br$: C, 56.84; H, 4.21; N, 7.80. Found: C, 56.79; H, 4.13; N, 7.56.

3.5 *Typical procedure for the trifluoroacetylation of* **2a–d** *and* **4a–d**

A mixture of **2**/**4** (1 equivalent) and TFAA (1.5 equivalent) in THF (15 mL/mmol of **1**/**4**) was heated at 60 °C for 5 h. The mixture was cooled to room temperature quenched with saturated sodium hydrogen carbonate solution. The mixture was extracted with chloroform (3 x 20 mL) and the combined organic layers were dried with anhydrous $MgSO_4$ and the salt was filtered off. The solvent was evaporated under reduced pressure and the residue was purified by column chromatography on a silica gel 20% or 60% EtOAc-hexane as eluent to afford **5a–d** or **5e–h** as a solids, respectively. Compounds **5a–h** were prepared in this fashion.

1-(7-Acetyl-5-bromo-2-phenyl-1H-indol-3-yl)- 2,2,2-trifluoroethanone (**4a**). A mixture of **2a** (0.30 g, 0.95 mmol) and TFAA (0.30 g, 1.43 mmol) in THF (15 mL) afforded **5a** as solid (0.30 g, 78%); R_f 0.86, mp. 175–176 °C; ν_{max} (ATR) 515, 647, 671, 697, 746, 767, 861, 911, 994, 1083, 1143, 1203, 1275, 1358, 1433, 1450, 1660, 3401 cm^{-1}; ^{1}H-NMR (DMSO-d_6) 2.70 (3H, s, CH_3), 7.47–7.55 (5H, m, Ph), 8.14 (1H, d, J = 1.2 Hz, 4-H), 8.42 (1H, d, J = 1.2 Hz, 6-H), 12.52 (1H, s, NH); ^{13}C-NMR (DMSO-d_6) 27.8, 107.3, 115.6, 116.2 (q, $^1J_{CF}$ 288.5 Hz), 123.7, 128.1, 128.3, 129.3, 130.4, 130.5 (2xC), 130.7, 132.3, 151.6, 176.6 (q, $^2J_{CF}$ 35.6 Hz), 198.3; m/z 410 (100, M+H); HRMS (ES): found 410.0015. $C_{18}H_{12}NO_2F_3^{79}Br^+$ requires 410.0003. *Anal* calcd for $C_{18}H_{11}NO_2F_3Br$: C, 52.71; H, 2.70; N, 3.41. Found: C, 52.62; H, 2.35; N, 3.39.

1-[7-Acetyl-5-bromo-2-(4-fluorophenyl)-1H-indol-3-yl]- 2,2,2-trifluoroethanone (**5b**). A mixture of **2b** (0.30 g, 0.90 mmol) and TFAA (0.28 g, 1.35 mmol) in THF (15 mL) afforded **5b** as solid (0.26 g, 69%); R_f 0.86, mp. 168–171 °C; ν_{max} (ATR) 518, 587, 645, 667, 706, 746, 842, 911, 999, 1082, 1142, 1205, 1244, 1274, 1435, 1489,

Preprints (www.preprints.org) | NOT PEER-REVIEWED | Posted: 4 May 2018 doi:10.20944/preprints201805.0085.v1

Peer-reviewed version available at Pharmaceuticals 2018, 11, 59; doi:10.3390/ph11020059

1606, 1662, 3401 cm^{-1}; ^{1}H-NMR (DMSO-d_6) 2.70 (3H, s, CH_3), 7.33 (2H, t, J 8.5 Hz, 3',5'-H), 7.62 (2H, t, J 6.9 Hz, 2',6'-H), 8.14 (1H, d, J = 1.2 Hz, 4-H), 8.42 (1H, d, J = 1.2 Hz, 6-H), 12.61 (1H, s, NH); ^{13}C-NMR (DMSO-d_6) 27.8, 107.4, 115.1 (d, $^2J_{CF}$ = 21.8 Hz), 115.7, 116.3 (q, $^1J_{CF}$ = 288.6 Hz), 123.6, 127.1 (d, $^4J_{CF}$ = 3.5 Hz), 128.4, 129.4, 130.3, 132.2, 133.2 (d, $^3J_{CF}$ = 8.0 Hz), 150.7, 163.6 (d, $^1J_{CF}$ = 246.2 Hz), 176.3 (q, $^2J_{CF}$ = 35.5 Hz), 198.3; m/z (100, M+H); HRMS (ES): found 427.9721. $C_{18}H_{11}NO_2F_4{}^{79}Br^+$ requires 427.9909. *Anal* calcd for $C_{18}H_{10}NO_2F_4Br$: C, 50.49; H, 2.35; N, 3.27. Found: C, 50.44; H, 2.31; N, 3.30.

1-[7-Acetyl-5-bromo-2-(3-chlorophenyl)-1H-indol-3-yl]-2,2,2-trifluoroethanone (**5c**). A mixture of **2c** (0.30 g, 0.86 mmol) and TFAA (0.27 g, 1.29 mmol) in THF (15 mL) afforded **5c** as solid (0.21 g, 56%); R_f 0.86, mp. 138–141 °C; ν_{max} (ATR) 581, 661, 702, 728, 769, 795, 870, 903, 913, 946, 997, 1074, 1147, 1209, 1281, 1316, 1433, 1462, 1651, 3257 cm^{-1}; ^{1}H-NMR (DMSO-d_6) 2.70 (3H, s, CH_3), 7.51–7.52 (2H, m, 4',5'-H), 7.60–7.62 (1H, m, 6'-H), 7.67 (1H, s, 2'-H), 8.15 (1H, d, J = 1.2 Hz, 4-H), 8.42 (1H, d, J = 1.2 Hz, 6-H), 12.72 (1H, s, NH); ^{13}C-NMR (DMSO-d_6) 27.9, 107.5, 115.7, 116.3 (q, $^1J_{CF}$ 288.6 Hz), 123.7, 128.4, 129.6, 129.7, 129.9, 130.1, 130.2, 130.5, 132.2, 132.6, 132.7, 149.9, 176.2 (q, $^2J_{CF}$ 35.5 Hz), 198.3; m/z 444 (100, M+H); HRMS (ES): found 443.9623. $C_{18}H_{11}NO_2F_3{}^{35}Cl^{79}Br^+$ requires 443.9614. *Anal* calcd for $C_{18}H_{10}NO_2F_3ClBr$: C, 48.62; H, 2.27; N, 3.15. Found: C, 48.47; H, 2.26; N, 2.98.

1-[7-Acetyl-5-bromo-2-(4-methoxyphenyl)-1H-indol-3-yl]-2,2,2-trifluoroethanone (**5d**). A mixture of **2d** (0.30 g, 0.87 mmol) and TFAA (0.27 g, 1.31 mmol) in THF (15 mL) afforded **5d** as solid (0.29 g, 75%); R_f 0.70, mp. 170–173 °C; ν_{max} (ATR) 615, 642, 660, 746, 836, 910, 1028, 1082, 1140, 1173, 1202, 1262, 1437, 1489, 1607, 1657, 3392 cm^{-1}; ^{1}H-NMR (DMSO-d_6) 2.70 (3H, s, CH_3), 3.83 (3H, s, OCH_3), 7.05 (2H, d, J = 8.7 Hz, 3',5'-H), 7.52 (2H, d, J = 8.7 Hz, 2',6'-H), 8.11 (1H, d, J = 1.2 Hz, 4-H), 8.38 (1H, d, J = 1.2 Hz, 6-H), 12.32 (1H, s, NH); ^{13}C-NMR (DMSO-d_6) 27.9, 107.0, 113.7, 115.5, 116.3 (q, $^1J_{CF}$ = 289.7 Hz), 122.8, 123.0, 123.5, 128.2, 129.2, 130.5, 132.2, 132.4, 151.8, 161.2, 176.7 (q, $^2J_{CF}$ = 35.6 Hz), 198.5; m/z 440 (100, M+H); HRMS (ES): found 440.0110. $C_{19}H_{14}NO_3F_3{}^{79}Br^+$ requires 440.0109. *Anal* calcd for $C_{19}H_{13}NO_3F_3Br$: C, 51.84; H, 2.98; N, 3.18. Found: C, 51.78; H, 2.93; N, 3.14.

N-[5-Bromo-2-phenyl-3-trifluoroacetyl-1H-indol-7-yl]acetamide (**5e**). A mixture of **4a** (0.30 g, 0.91 mmol) and TFAA (0.29 g, 1.37 mmol) in THF (15 mL) afforded **5e** as solid (0.32 g, 84%); R_f 0.49, mp. 141–144 °C; ν_{max} (ATR) 502, 582, 659, 699, 738, 773, 863, 882, 922, 1010, 1143, 1199, 1269, 1334, 1389, 1434, 1449, 1546, 1627, 1655, 3210, 3329 cm^{-1}; ^{1}H-NMR (DMSO-d_6) 2.11 (3H, s, CH_3), 7.53–7.63 (5H, m, Ar), 7.94 (1H, d, J = 1.2 Hz, 4-H), 7.96 (1H, d, J = 1.2 Hz, 6-H), 9.74 (1H, s, NH), 12.53 (1H, s, NH); ^{13}C-NMR (DMSO-d_6) 24.3, 107.2, 116.2, 116.6 (q, $^1J_{CF}$ = 295.5 Hz), 118.8, 126.2, 126.3, 126.8, 128.6, 129.5, 130.3, 130.6, 131.3, 149.2, 169.3, 175.9 (q, $^2J_{CF}$ = 35.6 Hz); m/z 425 (1000, M+H); HRMS (ES): found 425.0107. $C_{18}H_{13}N_2O_2F_3{}^{79}Br^+$ requires 425.0112. *Anal* calcd for $C_{18}H_{12}N_2O_2F_3Br$: C, 50.85; H, 2.84; N, 6.99. Found: C, 50.52; H, 2.87; N, 6.94.

N-[5-Bromo-2-(4-fluorophenyl)-3-trifluoroacetyl-1H-indol-7-yl]acetamide (**5f**). A mixture of **4b** (0.30 g, 0.86 mmol) and TFAA (0.27 g, 1.30 mmol) in THF (15 mL) afforded **5f** as solid (0.29 g, 78%); R_f 0.50, mp. 195–197 °C; ν_{max} (ATR) 515, 611, 732, 844, 884, 924, 1011, 1044, 1146, 1198, 1224, 1271, 1330, 1447, 1497, 1631, 1659, 3196, 3286 cm^{-1}; ^{1}H-NMR (DMSO-d_6) 2.12 (3H, s, CH_3), 7.41 (2H, t, J = 9.0 Hz, 3',5'-H), 7.69 (2H, d, J = 8.7 Hz, 2',6'-H), 7.93 (1H, d, J = 1.2 Hz, 4-H), 7.94 (1H, d, J = 1.2 Hz, 6-H), 9.77 (1H, s, NH), 12.54 (1H, s, NH); ^{13}C-NMR (DMSO-d_6) 24.2, 107.4, 115.7 (d, $^2J_{CF}$ 21.8 Hz), 116.1, 116.5 (q, $^1J_{CF}$ 288.6 Hz), 118.7, 118.8, 126.2, 126.9, 127.6 (d, $^4J_{CF}$ = 3.5 Hz), 129.4, 133.8 (d, $^3J_{CF}$ = 9.1 Hz), 148.2, 163.6 (d, $^1J_{CF}$ = 246.2 Hz), 169.3, 176.6 (q, $^2J_{CF}$ = 35.5 Hz); m/z 443 (100, M+H); HRMS (ES): found 443.0020. $C_{18}H_{13}N_2O_2F_4{}^{79}Br^+$ requires 443.0020. *Anal* calcd for $C_{18}H_{12}N_2O_2F_4Br$: C, 48.78; H, 2.50; N, .6.32. Found: C, 48.59; H, 2.39; N, 6.30.

Preprints (www.preprints.org) | NOT PEER-REVIEWED | Posted: 4 May 2018 doi:10.20944/preprints201805.0085.v1

Peer-reviewed version available at Pharmaceuticals 2018, 11, 59; doi:10.3390/ph11020059

N-[5-Bromo-2-(3-chlorophenyl)-3-trifluoroacetyl-1H-indol-7-yl]acetamide (**5g**). A mixture of **4c** (0.30 g, 0.83 mmol) and TFAA (0.26 g, 1.23 mmol) in THF (15 mL) afforded **5g** as solid (0.19 g, 52%); R_f 0.50, mp. 172–174 °C; ν_{max} (ATR) 541, 570, 685, 746, 794, 851, 913, 1010, 1039, 1083, 1143, 1198, 1260, 1369, 1441, 1542, 1630, 1660, 3217, 3356 cm^{-1}; ^{1}H-NMR (DMSO-d_6) 2.12 (3H, s, CH_3), 7.60–7.66 (3H, m, Ar), 7.75 (1H, s, 2′-H), 8.28 (1H, d, J = 1.2 Hz, 4-H), 8.29 (1H, d, J = 1.2 Hz, 6-H), 9.77 (1H, s, NH), 12.61 (1H, s, NH); ^{13}C-NMR (DMSO-d_6) 24.3, 107.4, 116.2, 116.5 (q, $^1J_{CF}$ = 289.7 Hz), 118.9, 126.3, 127.2, 129.3, 129.9, 130.5, 133.2, 133.4, 147.3, 169.3, 175.6 (q, $^2J_{CF}$ = 34.4 Hz); m/z 449 (100, M+H); HRMS (ES): found 458.9731. $C_{18}H_{12}F_3N_2O_2{}^{35}Cl^{79}Br^+$ requires 458.9723. *Anal* calcd for $C_{18}H_{11}F_3N_2O_2ClBr$: C, 47.03; H, 2.41; N, 6.09. Found: C, 47.10; H, 2.36; N, 6.05.

N-[5-Bromo-2-(4-methoxyphenyl)-3-trifluoroacetyl-1H-indol-7-yl]acetamide (**5h**). A mixture of **4d** (0.30 g, 0.83 mmol) and TFAA (0.26 g, 1.25 mmol) in THF (15 mL) afforded **5h** as solid (0.30 g, 80%); R_f 0.23, mp. 179–182 °C; ν_{max} (ATR) 520, 573, 643, 751, 838, 884, 922, 1009, 1031, 1154, 1191, 1250, 1415, 1448, 1499, 1538, 1629, 1645, 3211, 3369 cm^{-1}; ^{1}H-NMR (DMSO-d_6) 2.08 (3H, s, CH_3), 3.80 (3H, s, OCH_3), 7.07 (2H, d, J = 8.7 Hz, 3',5'-H), 7.52 (2H, d, J = 8.7 Hz, 2',6'-H), 7.86 (1H, d, J = 1.2 Hz, 4-H), 9.91 (1H, d, J = 1.2 Hz, 6-H), 9.74 (1H, s, NH), 12.39 (1H, s, NH); ^{13}C-NMR (DMSO-d_6) 24.2, 55.8, 107.0, 114.1, 116.0, 116.6 (q, $^1J_{CF}$ = 289.7 Hz),118.4, 118.6, 123.2, 126.3, 126.8, 129.6, 131.9, 149.5, 161.2, 169.2, 176.9 (q, $^2J_{CF}$ = 35.5 Hz); m/z 455 (100, M+H); HRMS (ES): found 455.0195. $C_{19}H_{15}N_2O_3F_3{}^{79}Br^+$ requires 455.0219. *Anal* calcd for $C_{19}H_{14}N_2O_3F_3Br$: C, 50.13; H, 3.10; N, 6.15. Found: C, 49.95; H, 3.20; N, 6.00.

3.6 Evaluation for cytotoxicity

3.6.1 Screening protocol

The human cervical cancer cell line, HeLa, and lung cancer cell line, A549 were used for the screening assay. HeLa cells were grown and maintained in RPMI 1640 medium supplemented with 10% foetal bovine serum (FBS) and A549 cells were grown and maintained in EMEM supplemented with 10% FBS and 10% non-essential amino acids. For a screening experiment, cells were seeded into 96 well microtiter plates at a density of 6000 cells/well using a volume of 200 µL in each well. The microtiter plates were incubated at 37 °C, 5% CO_2, and 100% relative humidity for 24 h prior to addition of test compounds to allow for cell attachment. Test compounds were first reconstituted in DMSO at a concentration of 40 mM and stored at 4 °C prior to use and final dilution to working concentrations with culture complete medium on the day of treatment. Two hundred microliters aliquots of the diluted compound in fresh medium was used to treat cells after aspiration of seeding medium. Both cell lines were incubated at 37 °C in a humidified 5% CO_2 incubator for 48 h. Treatment medium was aspirated from all wells and replaced with 100 µL of Hoechst 33342 nuclear dye (5 µg/mL) and incubated for 10 minutes at room temperature. Thereafter, cells were stained with propidium iodide (PI) at 100 µg/mL in order to enumerate the proportion of dead cells within the population. Cells were imaged immediately after addition of PI using the ImageXpress Micro XLS Widefield Microscope (Separations, Randburg, South Africa).

3.6.2 Dose response analysis and determination of IC_{50} values

Cells were seeded as described in above. The compounds were tested at a concentration range of 0–100 µM to determine their respective IC_{50} values on lung cancer (A549) cells and cervical cancer (HeLa) cells. The medium was aspirated and replaced with 200 µL fresh medium containing the dilution of the respective test compound. Following test sample addition, the plates were incubated for a further 48 h at 37 °C, 5% CO_2, in a humidified incubator. At the end of this incubation period the medium was removed

Preprints (www.preprints.org) | NOT PEER-REVIEWED | Posted: 4 May 2018 doi:10.20944/preprints201805.0085.v1

Peer-reviewed version available at Pharmaceuticals 2018, 11, 59; doi:10.3390/ph11020059

and replaced with 100 µL fresh culture medium containing MTT at a final concentration of 0.5 mg/mL. The 96-well plates were returned to the incubator and incubated for an additional 3 h following which the medium was removed. The MTT crystals were solubilised in 100 µL DMSO and the absorbance was measured at 560 nm using a Labsystems Multiwell Scanning spectrophotometer (Thermo Fischer Scientific, Edenvale, South Africa).

3.6.3 Data analysis

Quantification of live and dead cells for the screening assay was performed using the ImageXpress Micro XLS Widefield Microscope and acquired images analysed using the MetaXpress software and Multi-Wavelength Cell Scoring Application Module. Acquired data was transferred to an EXCEL spreadsheet and relative cell viability was determined using quadruplicate wells for each concentration. Untreated cells were considered to have 100% cell viability (i.e., the mean OD of the untreated wells = 100% viability). Cell viabilities in other test wells were calculated relative to the untreated control and expressed as a percentage. Dose response analysis was performed using the statistical software GraphPad Prism and IC_{50} values calculated from the concentration-response data using a mathematical Hill function. If the concentration range selected did not produce 100% inhibition, a lower concentration equal to zero was included to allow IC_{50} determination.

3.7 Evaluation of mode of cell death

3.7.1 Caspace activation

Compounds **4c** and **5g** were selected for mechanism studies and these test compounds were reconstituted in dimethyl sulphoxide (DMSO) to give a final concentration of 40 mM. Samples were stored at 4 °C until required. Cells were seeded and treated as described in 4.3.1. Cells were first fixed and permeabilized using the IntraPrep kit as per manufacturer's instructions (Beckman Coulter). This kit allows for the immunological detection of intracellular antigens by creating apertures in the cell membrane without affecting the morphology of the cell. Cleaved caspase-8 (Asp 391) and cleaved caspase-3 (Asp 175) monoclonal antibodies (Cell Signaling Technology) were used to determine the presence of activated caspase-8 and caspase-3, respectively. Cells were first blocked using PBS containing 0.5% BSA and thereafter incubated with the antibodies separately (1:200 for caspase-8 and 1:100 for caspase-3) for 1 h at 37 °C. Cells were washed and incubated with the Alexa 647 conjugated secondary antibody (1:1000) for 30 minutes at 37 °C in the dark. Both cell lines were incubated at 37 °C in a humidified 5% CO_2 and then treated with the IC_{50} values of each compound for 24 h. 200 µL Aliquots of the diluted compound in fresh medium was used to treat cells after aspiration of seeding medium. Treatment medium was aspirated from all wells and replaced with 100 µL of Hoechst 33342 nuclear dye (5 µg/mL) and incubated for 10 minutes at RT.

3.7.2 Data quantification

Quantification of live and dead cells for the assay was performed using the ImageXpress Micro XLS Widefield Microscope and acquired images analysed using the MetaXpress software and Multi-Wavelength Cell Scoring Application Module and the Cell Cycle Module. Acquired data was transferred to an EXCEL spreadsheet and data was analysed and processed.

3.8 Tubulin Polymerization Assay

Tubulin polymerization assays were conducted using the tubulin polymerization assay kit following the manufacturer's instructions (Cytoskeleton, Inc.). Briefly, 50 µL of 1.3 mg/mL tubulin (>99% pure) proteins in G-PEM buffer (80 mmol/L PIPES, pH 6.9, 2 mmol/L $MgCl_2$, 0.5 mmol/L EGTA, 1 mmol/L GTP,

Preprints (www.preprints.org) | NOT PEER-REVIEWED | Posted: 4 May 2018 doi:10.20944/preprints201805.0085.v1

Peer-reviewed version available at Pharmaceuticals 2018, 11, 59; doi:10.3390/ph11020059

and 15% glycerol) was placed in a quartz cuvette in the presence of the test agent (concentration: 0.25 μM). Polymerization was measured at every 3 seconds for 1 h using an Applied Photophysics Chirascan spectroflourimeter (excitation at 360 nm and emission at 420 nm) at 37 °C.

3.9 Methodology for Docking Studies

Molecular docking of compounds **2a**, **4a** and **5e–h** to the 3D structure of a tubulin heterodimer (PDB code:1TUBE [30] was carried out using the CDOCKER protocol [31] in Discovery Studio 2017. Prior to performing the docking, compounds were drawn using Discovery Studio and prepared using the 'Prepare Ligand' protocol. The protein structure was downloaded from the Protein Data Bank, prepared using the 'Prepare Protein' protocol in Discovery Studio which included removing any existing ligands bound to the model and binding sites defined from receptor cavities. The receptor cavity in this tubulin structure is present between the two monomers of the tubulin dimer structure. Docking was performed using default settings and the best conformation of the ligand selected and evaluated.

4. Conclusions

The observed increased cytotoxicity of compounds **5e–h** against the A549 and HeLa cell lines and their strong inhibitory effect against tubulin polymerization suggest that a combination of the strong hydrogen bonding 7-acetamido and the 3-trifluoroacetyl groups on the 2-aryl-5-bromoindole framework is desirable for biological activity. An acetamido group elicited some cytotoxicity in derivatives **4b–d** against both cell lines, which increased significantly upon incorporation of a trifluoroacetyl group in **5e–h**. This observation suggest the importance of a nitrogen-based substituent on the fused benzo ring of indole derivatives in analogy with the literature precedence on the increased cytotoxicity of analogues indoles against the HeLa and A549 cell lines as well as HIV-1 inhibition activity [6]. The lack of cytotoxicity for the C-3 unsubstituted 2-arylindoles **2a-d** or their 3-trifluoroacetyl derivatives **5a–d** in our view suggest that the presence of an acetyl group on the fused benzo ring is undesirable for biological activity of the 2-arylindoles. The immunochemical experiments, on the other hand, revealed that the 3-trifluoroacetyl derivatives **5e–h** may induce apoptosis in a caspase-dependent manner for both cell lines. Experimental and molecular docking of **5e–h** into the colchicine-binding site of tubulin suggest that these compounds have potential to inhibit tubulin polymerization to elicit anticancer activity. The binding of these compounds to tubulin would in our view prevent tubulin polymerization or disassociation and probably induce apoptosis. These results pave the way for the development of the 3-trifluoroacetyl substituted indole derivatives as anticancer agents.

Supplementary Materials: The following materials are available online. Copies of ^{1}H- & ^{13}C-NMR spectra for compounds **2a–d**, **3a–d**, **4a–d** and **5a–h** (Figure S1), % cell viability for compounds of **2a–d**, **4a–d** and **5a–h** (Figure S2), dose response curves for compounds **5e–h** (Figure S3) and spread sheet for statistical analysis which contains p values for each test (Figure S4).

Author Contributions: MJM coordinated the study, reviewed the literature, interpreted the data and results, and written the manuscript. NP assayed the compounds for inhibitory effects against tubulin polymerization and performed molecular docking studies.

Acknowledgments: The authors are grateful to the University of South Africa and the National Research Foundation for financial assistance. We thank the University of Stellenbosch Central Analytical Facility (CAF) for mass spectrometric and elemental analyses. We also acknowledge the technical assistance of M.M. Mmonwa and M.M.

Preprints (www.preprints.org) | NOT PEER-REVIEWED | Posted: 4 May 2018 doi:10.20944/preprints201805.0085.v1

Peer-reviewed version available at Pharmaceuticals 2018, 11, 59; doi:10.3390/ph11020059

Maluleka as well as Prof M. Van De Venter and Dr L. Venables of the Nelson Mandela Metropolitan University (Summerstrand Campus South) for the *in vitro* cytotoxicity assays.

Conflicts of Interest: The authors declare no conflict of interest.

References

1. Lu, Y.; Chen, J.; Xiao, M.; Li W.; Miller, D.D. An overview of tubulin inhibitors that interact with the colchicine binding site. *Pharm. Res.* **2012**, *29*, 2943–2971.
2. Jordan, M.A. Anti-cancer agents. *Curr. Med. Chem.* **2002**, *2*, 1–17.
3. Gastpar, R.; Goldbrunner, M.; Marko, D.; Von Angerer, E.; Methoxy-substituted 3-formyl-2-phenylindoles inhibit tubulin polymerization. *J. Med. Chem.* **1998**, *41*, 4965–4972.
4. Dong, M.; Liu, F.; Zhou, H.; Zhai, S.; Yan, B. Novel natural product- and privileged scaffold-based tubulin inhibitors targeting the colchicine binding site. *Molecules* **2016**, *21*, 1375–1400.
5. Kaur, R.; Kaur, G.; Gill, R.K.; Soni, R.; Bariwal, J. Recent developments in tubulin polymerization inhibitors: an overview. *Eur. J. Med. Chem*. **2014**, *87*, 89–124.
6. Hu, H.; Wu, J.; Ao, M.; Wang, H.; Zhou, T.;, Xue, Y.; Qiu, Y.; Fang, M.; Wu, Z. Synthesis, structure–activity relationship studies and biological evaluation of novel 2,5-disubstituted indole derivatives as anticancer agents. *Chem. Biol. Drugs Des*. **2016**, *88*, 766–778.
7. Cooper, L.C.; Chicchi, G.G.; Dinnell, K.; Elliott, J.M.; Hollingworth, G.J.; Kurtz, M.M.; Locker, K.L.; Morrison, D.; Shaw, D.E.; Tsao, K.-L.; Watt, A.P.; Williams, A.R.; Swain, C.J. 2-Aryl indole NK1 receptor antagonists: optimisation of indole substitution. *Bioorg. Med. Chem. Lett*. 2001, *11*, 1233–1236.
8. Sisa, M.; Pla, D.; Altuna, M.; Francesch, A.; Cuevas, C.; Albericio, F.; Alvarez, M. Total synthesis and antiproliferative activity screening of (±)-Aplicyanins A, B and E and related analogues. *J. Med. Chem.* **2009**, *52*, 6217–6223.
9. Watterson, S.H.; Dhar, T.G.M.; Ballentine, S.K.; Shen, Z.; Barrish, J.C.; Cheney, D.; Fleener, C.A.; Roleau, K.A.; Townsend, R.; Hollenbaugh, D.L.; Iwanovicz, E.J. Novel indole-based inhibitors of IMPDH: introduction of hydrogen bond acceptors at indole C-3. *Bioorg. Med. Chem. Lett*. **2003**, *13*, 1273–1276.
10. Thomas, J.B.; Giddings, A.M.; Wiethe, R.W.; Olepu, S.; Warner, K.R.; Sarret, P.; Gendron, L.; Longpre, J.-M.; Zhang, Y.; Runyon, S.P.; Gilmour, B.P. Identification of *N*-[(5-{[(4-methylphenyl)sulfonyl]amino}-3-(trifluoroacetyl)-1*H*-indol-1-yl)acetyl]-L-leucine (NTRC-824), a neurotensin-like nonpeptide compound selective for the neurotensin receptor type 2. *J. Med. Chem.* **2014**, *57*, 7472–7477.
11. Usachev, B.I. 1-/2-/3-Fluoroalkyl-substituted indoles, promising medicinally and biologically beneficial compounds: synthetic routes, significance and potential applications. *J. Fluorine. Chem*. **2016**, *185*, 118–167.
12. Cade, H.C.; Blocker, M.; Shaik, A. Synthesis of indole-derived fluorine-containing amino acids. J. Nat. Sci. **2015**, *1*, e169.
13. Lo´pez, S.E.; Salazar, J. Trifluoroacetic acid: uses and recent applications in organic synthesis. *J. Fluorine Chem*. **2013**, *156*, 73–100.

Preprints (www.preprints.org) | NOT PEER-REVIEWED | Posted: 4 May 2018 doi:10.20944/preprints201805.0085.v1

Peer-reviewed version available at Pharmaceuticals 2018, 11, 59; doi:10.3390/ph11020059

14. Mphahlele, M.J.; Mmonwa, M.M.; Makhafola, T.J. In vitro cytotoxicity of novel 2,5,7-tricarbo-substituted indoles derived from 2-amino-5-bromo-3-iodoacetophenone. *Bioorg. Med. Chem*. **2016**, *24*, 4576–4586.
15. Choi, H.-S.; Cho, M.-C.; Lere, H.G.; Yoon, D.-Y. Indole-3-carbinol induces apoptosis through p53 and activation of caspase-8 pathway in lung cancer A549 cells. *Food Chem. Tox.* **2010**, *48*, 883–890.
16. Mphahlele, M.J.; Maluleka, M.M.; Trifluoroacetylation of indole-chalcones derived from the 2-amino-3-(arylethynyl)-5-bromo-iodochalcones. *J. Fluorine Chem*. **2016**, *189*, 88–95.
17. Mphahlele, M.J.; Mmonwa, M.M.; Choong, Y.S. Synthesis and evaluation of *N*-(3-trifluoroacetyl-indol-7-yl)acetamides for potential in vitro antiplasmodial properties. *Molecules* **2017**, *22*, 1099–1115.
18. Yao, S.-J.; Ren, Z.-H.; Wang, Y.-Y.; Guan, Z.-H.; Friedel–Crafts fluoroacetylation of indoles with fluorinated acetic acids for the synthesis of fluoromethyl indol-3-yl ketones under catalyst- and additive-free conditions. *J. Org. Chem*. **2016**, *81*, 4226–4234.
19. Owa, T.; Yokoi, A.; Yamazaki, K.; Yoshimatsu, K.; Yamori, T.; Nagasu, T. Array-based structure and gene expression relationship study of antitumor sulfonamides including *N*-[2-[(4-hydroxyphenyl)amino]-3-pyridinyl]-4-methoxybenzenesulfonamide and *N*-(3-chloro-7-
20. indolyl)-1,4-benzenedisulfonamide. *J. Med. Chem*. **2002**, *45*, 4913–4922.
21. Choi, H.-S.; Cho, M.-C.; Lere, H.G.; Yoon, D.-Y.; Indole-3-carbinol induces apoptosis through p53 and activation of caspase-8 pathway in lung cancer A549 cells. *Food Chem. Tox.* **2010**, *48*, 883–890.
22. Kroemer, G.; Galluzzi, L.; Vandenabeele, P.; Abrams, J.; Alnemri, E.S.; Baehrecke, E.H.; Blagosklonny, M.V.; El-Deiry, W.S.; Golstein, P.; Green D.R.; Hengartner, M.; Knight, R.A.; Kumar, S.; Lipton, S.A.; Malorni, W.; Nunez, G.; Peter, M.E.; Tschopp, J.; Yuan, J.; Piacentini, M.; Zhivotovsky, B.; Melino, G. Classification of cell death: recommendations of the Nomenclature Committee on Cell Death 2009. *Cell Death Diff.* **2009**, *16*, 3–11.
23. Fischer, U.; Janicke, R.U.; Schulze-Osthoff, K. Many cuts to ruin: a comprehensive update of caspase substrates. *Cell Death Differ*. **2003**, *10*, 76–100.
24. Fulda, S.; Debatin, K.-A. Extrinsic versus intrinsic apoptosis pathways in anticancer chemotherapy. *Oncogene* **2006**, *25*, 4798–481.
25. Taylor, R.C.; Cullen S.P.; Martin, S.J. Apoptosis: controlled demolition at the cellular level. Nature Rev Mol. Cell Biol. **2008**, *9*, 231–241.
26. Cohen, G.M. Caspases; the executioners of apoptosis. *Biochem. J.* **1997**, *326*, 1–16.
27. Kool, E.T. Hydrogen bonding, base stacking, and steric effects in DNA replication. *Annu. Rev. Biophys. Biomol. Struct*. **2001**, *30*, 1–22.
28. Kumar, S.; Mehndiratta, S.; Nepali, K.; Gupta, M.K.; Koul, S.; Sharma, P.R.; Saxena, A.K.; Dhar, K.L. Novel indole-bearing combretastatin analogues as tubulin polymerization inhibitors. *Org. Med. Chem. Lett.* **2013**, *3*, http://www.orgmedchemlett.com/content/3/1/3.
29. Hadzi, D.; Kidric, J.; Koller, J.; Mavri, J. The role of hydrogen bonding in drug-receptor interactions. *J. Mol. Struct*. **1990**, *237*, 139–150.
30. Nogales, E.; Wolf, S.G.; Downing K.H. Structure of the β-tubulin dimer by electron crystallography. *Nature* **1998**, *391*, 199–203.

Preprints (www.preprints.org) | NOT PEER-REVIEWED | Posted: 4 May 2018 doi:10.20944/preprints201805.0085.v1

Peer-reviewed version available at Pharmaceuticals 2018, 11, 59; doi:10.3390/ph11020059

31. Wu, G.; Robertson, D.H.; Brooks III, C.L.; Vieth, M. Detailed analysis of grid-based molecular docking: a case study of CDOCKER—CHARMm-based MD docking algorithm. *J. Comput. Chem.* **2003**, *24*, 1549–1562.